

# Awesome Quantum Computing Experiments: Benchmarking Experimental Progress Towards Fault-Tolerant Quantum Computation

François-Marie Le Régent  
 Pasqal  
[francois-marie.le-regent@pasqal.com](mailto:francois-marie.le-regent@pasqal.com)

## Abstract

Achieving fault-tolerant quantum computation (FTQC) demands simultaneous progress in physical qubit performance and quantum error correction (QEC). This work reviews and benchmarks experimental advancements towards FTQC across leading platforms, including trapped ions, superconducting circuits, neutral atoms, NV centers, and semiconductors. We analyze key physical metrics like coherence times, entanglement error, and system size (qubit count), fitting observed exponential trends to characterize multi-order-of-magnitude improvements over the past two decades. At the logical level, we survey the implementation landscape of QEC codes, tracking realized parameters  $[[n, k, d]]$  and complexity from early demonstrations to recent surface and color code experiments. Synthesizing these physical and logical benchmarks reveals substantial progress enabled by underlying hardware improvements, while also outlining persistent challenges towards scalable FTQC. The experimental databases and analysis code underpinning this review are publicly available at <https://github.com/francois-marie/awesome-quantum-computing-experiments>.

## Table of contents

<b>1</b>	<b>Introduction</b>	<b>2</b>
<b>2</b>	<b>Physical Qubit Benchmarks</b>	<b>2</b>
2.1	Physical Platforms and Qubit Encoding . . . . .	3
2.2	Physical Level Metrics . . . . .	3
2.2.1	Bitflip and Coherence times . . . . .	3
2.2.2	Entanglement Error . . . . .	5
2.2.3	Qubit Count for Scale up . . . . .	6
<b>3</b>	<b>QEC Code Implementation</b>	<b>7</b>
3.1	Concept of QEC . . . . .	7
3.2	Experiments Considered . . . . .	8
3.3	Logical Level Metrics . . . . .	8
3.3.1	Cumulative Growth and Platform Distribution . . . . .	9
3.3.2	$[[n, k, d]]$ Representation . . . . .	9
3.3.3	QEC Performance Benchmarks . . . . .	10
<b>4</b>	<b>Conclusion</b>	<b>11</b>
<b>5</b>	<b>Acknowledgements</b>	<b>11</b>
<b>6</b>	<b>References</b>	<b>12</b>
<b>7</b>	<b>Appendices</b>	<b>23</b>
7.1	Reaching the Utility Scale . . . . .	23
7.2	Additional Visualisations . . . . .	24
7.2.1	Yearly Experiment Counts by Platform . . . . .	24
7.2.2	Cumulative Growth of QEC Implementations by Code Family . . . . .	24
7.2.3	Timeline of Implementations . . . . .	25

7.2.4	Distribution of Implementations Across Platforms and Codes . . . . .	25
7.3	Goodness of Fit for Exponential Trends . . . . .	26
7.3.1	Methodology . . . . .	26
7.3.2	Results . . . . .	27
7.3.3	Discussion . . . . .	29

## 1 Introduction

The realization of algorithms offering quantum advantage [1–4] demands quantum processors operating not just with a large number of qubits [5–8], but with qubits exhibiting high fidelity, often called “algorithmic qubits” (qubits meeting the fidelity requirements for useful algorithms) [9, 10]. Early physical qubit implementations [11–13], while demonstrating fundamental quantum phenomena, suffered from significant error rates, far exceeding the requirements for complex computations [14, 15]. The primary strategy to bridge this gap lies in quantum error correction (QEC) [14, 16, 17], where quantum information is redundantly encoded across multiple physical qubits to protect it from local errors, effectively creating robust logical qubits.

Progress towards fault-tolerant quantum computation [18–23] is thus intrinsically multi-faceted, requiring simultaneous improvements across all layers of the hardware stack. Key areas include extending the fundamental lifetimes ( $T_1$ ) and coherence times ( $T_2$ ) of physical qubits, minimizing errors in single- and multi-qubit gate operations, dramatically increasing the number of addressable and interconnected physical qubits, and successfully implementing and scaling QEC codes of increasing complexity and distance.

While individual metrics offer valuable insights into specific aspects of a given quantum computing platform’s maturity [24], a holistic view combining physical-level benchmarks with logical-level QEC implementation progress [25] is crucial for evaluating the trajectory towards fault tolerance and utility scale. The primary aim of this paper is therefore to present and analyze key performance metrics derived from experimental realizations of both physical qubit and QEC implementations. To provide the necessary context for interpreting these metrics, we first review the essential concepts at the physical qubit level for various platforms and their associated metrics in Section 2 followed by an overview of QEC principles and experimental code implementations at the logical level in Section 3 analyzing trends in complexity, and the platforms used.

Given the rapid pace of experimental advancement in the field, tracking progress requires dynamic tools. To facilitate ongoing tracking and analysis of this rapid progress, we have developed an open-source repository containing the databases of experimental results underpinning this review. This resource, available at <https://github.com/francois-marie/awesome-quantum-computing-experiments>, is designed to be easily updated by the community with new publications [26]. Adding new experimental realizations allows for the automatic regeneration of the figures presented herein, providing a continuously evolving snapshot of the state-of-the-art in physical qubit performance and QEC implementation across different platforms and codes.

Therefore, this work provides the following three key advances: (1) A unified benchmarking framework aggregating physical and logical qubit metrics across platforms, (2) Characterization of platform-specific improvement trends through analysis of 25-year experimental data, and (3) Open-source repository enabling tracking of documented quantum experiments through community contributions.

## 2 Physical Qubit Benchmarks

This section delves into the fundamental building blocks of quantum processors: the physical qubits. As outlined by Nielsen and Chuang [27], the physical realization of quantum computation necessitates fulfilling four fundamental requirements: robustly representing quantum information, performing a universal family of unitary transformations, state preparation, and measurement. Within this context, critical metrics for assessing performance include the robustness of quantum states against environmental noise, often quantified by  $T_1$  and  $T_2$  coherence times, and the precision in implementing quantum operations, particularly concerning the controllability required to generate and manipulate entangled states accurately.

We will thus examine key benchmarks used to assess the quality and progress of qubits across various leading experimental platforms [24, 28–31]. We begin by outlining the platforms considered and the basic concept of how quantum information is encoded within these physical systems. We will then analyze the physical-level metrics that

quantify performance, including qubit stability via  $T_1$  and  $T_2$  times, the fidelity of multi-qubit operations through entanglement error, and the progress towards large-scale systems indicated by physical qubit counts.

## 2.1 Physical Platforms and Qubit Encoding

To provide essential context for the analysis of performance metrics in this section, we briefly outline the physical encoding of quantum information within the hardware platforms considered. Our focus targets platforms demonstrating significant experimental progress towards QEC implementation. These include trapped ion systems [28, 32], various superconducting circuits [24, 33], neutral atoms held in dipole traps [29], Nitrogen vacancy (NV) centers [31] and semiconductors [30].

Quantum information is fundamentally encoded in the state of two-level quantum systems, known as qubits. The choice of which two levels within a larger physical system's Hilbert space represent the computational basis states  $|0\rangle$  and  $|1\rangle$  varies significantly across different hardware platforms, each choice presenting distinct advantages and challenges concerning qubit stability, control fidelity, readout efficiency, and scalability potential.

For instance, both trapped ions [28, 32] and neutral atoms held in dipole traps [29] commonly encode qubits in specific internal electronic energy levels. Often, two stable hyperfine ground states are selected, leveraging their long intrinsic lifetimes. Manipulation in trapped ions, which uses specific ionic species, typically involves precisely tuned microwave fields or lasers (depending on whether hyperfine or optical transitions are used). Neutral atoms, trapped using laser light (e.g., optical tweezers), also use laser or microwave fields for control, frequently employing highly excited Rydberg states to mediate strong interactions required for multi-qubit gates. While both platforms leverage atomic energy levels, the charged nature of ions allows for strong confinement via electric fields, whereas neutral atoms rely on trapping via induced dipole moments which can be accomplished with optical potentials.

Distinctly, superconducting circuits [24, 33] realize qubits not within natural atoms, but as the two lowest quantized energy eigenstates of macroscopic electrical circuits incorporating non-linear elements like Josephson junctions. These engineered “artificial atoms” (e.g., transmons, fluxoniums) have customizable energy level structures, with  $|0\rangle$  and  $|1\rangle$  corresponding to distinct energy levels manipulated primarily by microwave pulses. More complex encodings using higher energy levels or multiple circuit modes (bosonic codes) offer alternative pathways within this platform.

Another major approach displayed in the metrics of this section relies on spin degrees of freedom. NV centers [31], which are point defects within a diamond lattice, typically encode the qubit in the electron spin ground state, and control is achieved via microwave fields. The inherent solid-state environment also allows nearby nuclear spins, such as those of the Nitrogen atom forming the NV center itself (typically  $^{14}\text{N}$  or  $^{15}\text{N}$ ) or nearby carbon-13 atoms ( $^{13}\text{C}$ ) naturally present within the diamond lattice, to serve as qubits or long-lived memories, often offering longer coherence times than the NV electron spin. Similarly leveraging spin in a solid-state environment, semiconductor qubits [30] typically encode information in the spin state (spin-up  $|\uparrow\rangle$  representing  $|0\rangle$  and spin-down  $|\downarrow\rangle$  representing  $|1\rangle$ , or vice-versa) of individual charge carriers (electrons or holes) confined in nanoscale structures like quantum dots, or alternatively, using the nuclear or electron spin of donor atoms (e.g., phosphorus) implanted in a host material like silicon. While both NV centers and semiconductor qubits utilize spin, they differ significantly in their host material and the specific nature of the spin carrier (defect electron spin vs. confined electron/hole or donor spin).

As we will see in the next section, each encoding strategy profoundly influences the qubit's characteristics, including its susceptibility to different noise sources.

## 2.2 Physical Level Metrics

Evaluating the hardware platforms requires quantifiable benchmarks. We now detail several key metrics commonly used to characterize the quality of individual physical qubits and the scale of experimental systems.

### 2.2.1 Bitflip and Coherence times

The stability of a physical qubit is fundamentally limited by two characteristic times: the energy relaxation time ( $T_1$ , or bitflip time) and the dephasing time ( $T_2$ , or coherence time).  $T_1$  quantifies the timescale over which the system incoherently exchanges energy with its environment. However, the practical factor limiting this timescale can vary by platform. For example, in neutral atom qubits where the intrinsic decay between the hyperfine qubit states used is often negligible, the relevant timescale analogous to  $T_1$  is typically determined by off-resonant scattering of trapping light rather than spontaneous emission between  $|1\rangle$  and  $|0\rangle$ . Nevertheless, for the purpose of comparative analysis in this review, such dominant qubit loss timescales are generally categorized and plotted under the  $T_1$

## Physical Qubit Coherence Times Evolution

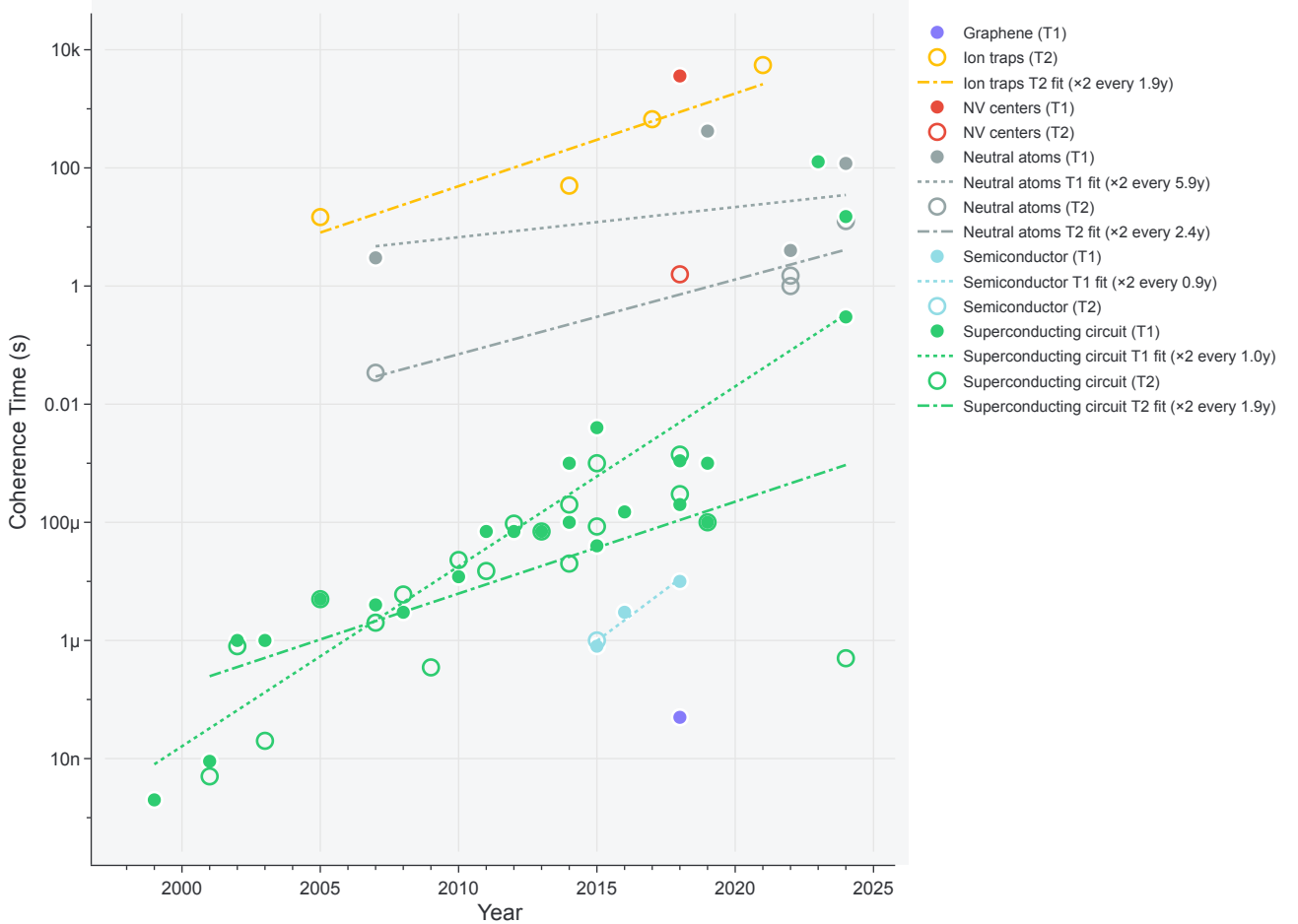


Figure 1: **Physical qubit bitflip and coherence times.** Evolution of reported  $T_1$  (solid lines) and  $T_2$  (dashed lines) times across different platforms. An exponential fit showing the characteristic doubling time in years is included. The platforms, ordered by their doubling time (fastest first), are: Semiconductor  $T_1$  (0.9y but only three data points are displayed), Superconducting circuit  $T_1$  (1.0y), Ion traps  $T_2$  (1.9y), Superconducting circuit  $T_2$  (1.9y), Neutral atoms  $T_2$  (2.4y), and Neutral atoms  $T_1$  (5.9y). See Section 7.3 for additional details on the fits.

metric.  $T_2$  measures the timescale over which the relative phase between  $|0\rangle$  and  $|1\rangle$  in a superposition state is lost. Long  $T_1$  and  $T_2$  times are essential for preserving quantum information.

The [physical\\_qubits](#) dataset [26] compiles this key information on physical qubits developed from 1999 to 2024, documenting their evolution across various platforms. For each experiment, the dataset records the code name, the corresponding research article title and link, the publication year, the platform type, and the coherence metrics including  $T_1$  and  $T_2$  times. Figure 1 plots this data, illustrating significant improvements over the past decades, particularly for superconducting circuits [24]. References are, in chronological order, for superconducting circuits [24] based on Josephson junctions [13, 34–52], and based on bosonic encodings [39, 47, 48, 50, 51, 53–56], for semiconductors [57–59], for trapped ions [60–63], for neutral atoms [64–68] and for graphene [69]. The last two decades have seen substantial improvements in physical qubit stability, with typical coherence times increasing by one or more orders of magnitude in several leading experimental platforms. Exponential fits to this data (see Section 7.3 for goodness-of-fit analysis) reveal characteristic doubling times ranging from approximately 0.9 years for semiconductor  $T_1$  to around 5.9 years for neutral atom  $T_1$ . It should be noted that for the superconducting circuit platform in particular, this overall trend analysis combines data from distinct qubit encodings, such as transmons and those based on bosonic codes, which inherently possess different characteristics and may exhibit varied individual

scaling trajectories but they are fitted collectively here for simplicity.

### 2.2.2 Entanglement Error

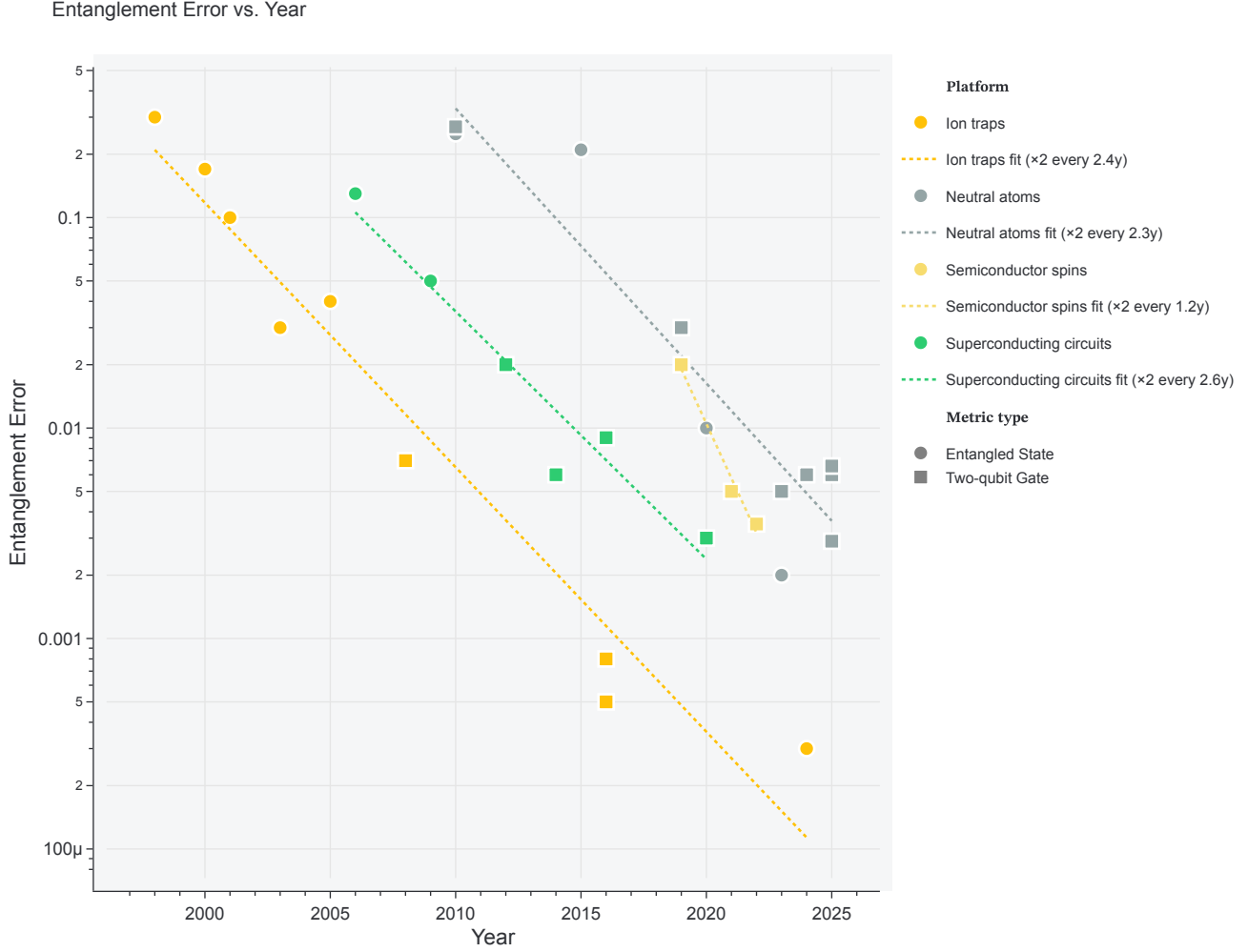


Figure 2: **Entanglement error.** Data points represent experimental achievements for ion traps (yellow circles), NV centers (red circle), neutral atoms (grey circles), semiconductor spins (light yellow circles), and superconducting circuits (green circles). Dotted lines show exponential fits to the data for platforms with sufficient data, indicating the approximate time required to halve the error rate: Semiconductor spins (1.2y), Neutral atoms (2.3y), Ion traps (2.4y), and Superconducting circuits (2.6y). See Section 7.3 for additional details on the fits.

Beyond single-qubit stability, the ability to create high-fidelity multi-qubit entanglement is paramount for quantum computation and QEC. For the purpose of this analysis and depending on the available data, we consider both Bell state preparation error (the error associated with generating a maximally entangled state) and two-qubit gate error as equivalent metrics for quantifying entanglement error, as both provide a measure of the system's ability to create and manipulate entangled states. The `entangled_state_error_exp` dataset tracks the evolution of error rates in entanglement across multiple quantum computing platforms from 1998 to 2025. For each experiment, the dataset records the entanglement error rate (entangled state error or two-qubit gate error), corresponding research article title, publication year, and implementation platform. Figure 2 plots the reported entanglement error over time for leading platforms. The references are, in chronological order, for superconducting circuits [70–75], for neutral atoms [76–86], for trapped ions [12, 87–94], for semiconductor spins [95–97] and for NV center [98]. We observe a consistent trend of decreasing entanglement error across ion traps, neutral atoms, and superconducting circuits, all below the sub-percent level. Exponential fits to the data indicate characteristic error halving times ranging from

approximately 1.2 years for semiconductor spins to 2.6 years for superconducting circuits, reflecting a consistent trend of rapid improvement over the past years (see Section 7.3 for more details). However, recent experimental results are above their respective fits which indicates that progress seems to be recently slowing down for ion traps, superconducting circuits and neutral atoms.

### 2.2.3 Qubit Count for Scale up

Achieving fault tolerance requires a large number of physical qubits to encode logical information and perform QEC [5, 6]. Scaling the number of individually controllable, high-quality qubits is therefore a major engineering challenge. The qubit count metric serves thus as a critical link between physical qubit progress and the resources available for implementing QEC codes. It is important to note that for neutral atom platforms, while trapping large numbers of atoms in optical lattices is relatively straightforward, the reported qubit counts specifically refer to systems demonstrating essential quantum computing capabilities such as site-resolved readout and internal-state manipulation, rather than just the raw number of trapped atoms. The [qubit\\_count](#) dataset displays experiments from 1998 to 2024, tracking the increasing number of qubits in experimental quantum systems across various platforms. For each realization, the dataset records the qubit count, corresponding research article title, publication year, and implementation platform.

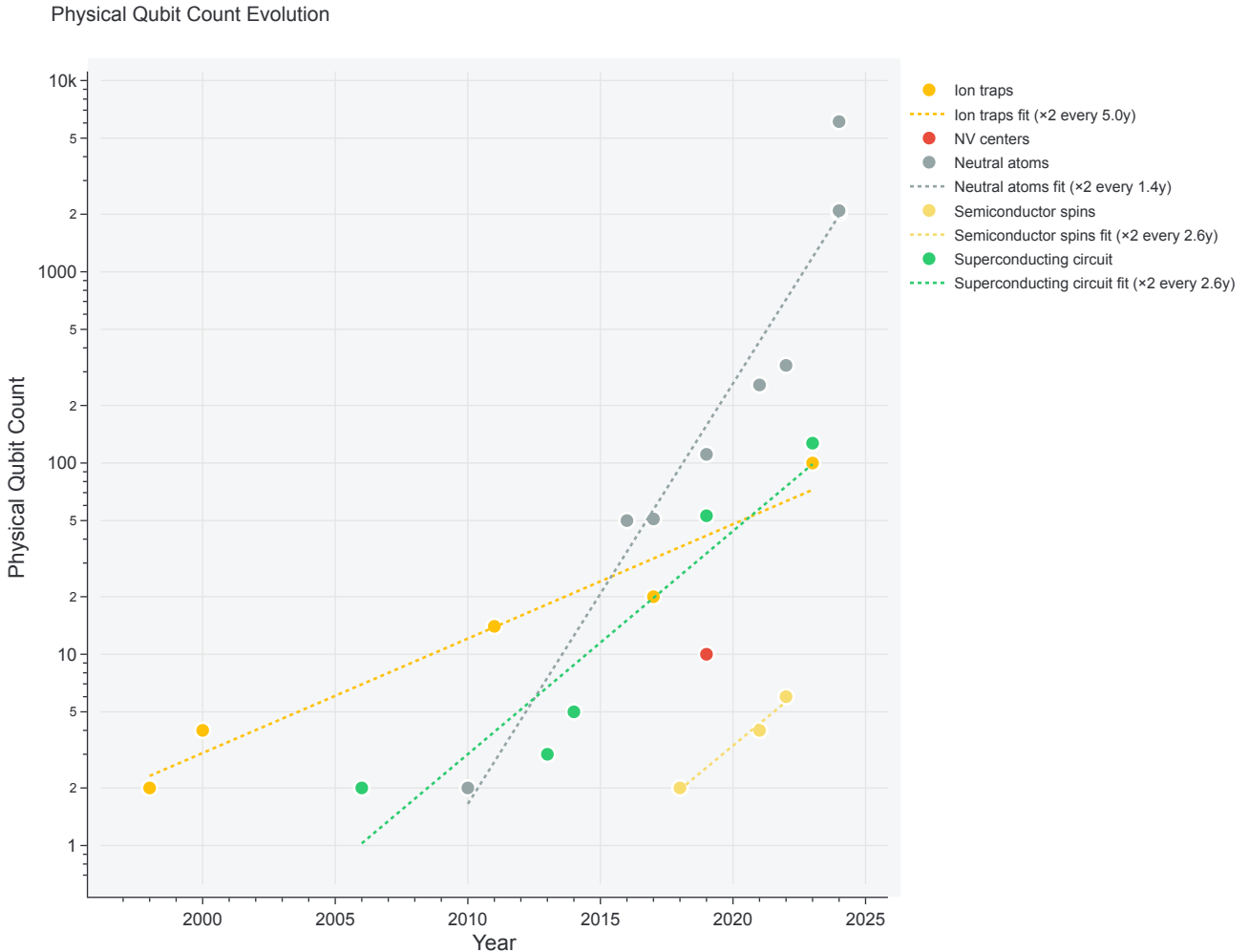


Figure 3: **Physical qubit count.** Maximum number of physical qubits reported in experiments over time for selected platforms. The color code is the same as in Figure 2. Dotted lines indicate exponential fits, showing the approximate doubling time for qubit count: Neutral atoms (1.4y), Superconducting circuits (2.6y), Semiconductor spins (2.6y), and Ion traps (5.0y). See Section 7.3 for additional details on the fits.

Figure 3 illustrates the growth in the maximum number of physical qubits reported. The references are, in chronological order, for ion traps [12, 87, 99–101], neutral atoms [68, 77, 102–108], superconducting circuit [70, 109–112], semiconductor spins [113–115], and NV centers [116]. The data highlights platform-specific scaling trajectories, with neutral atoms demonstrating the largest qubit counts (6,100 qubits), followed by superconducting circuits (127 qubits), and ion traps (100 qubits). Fitting exponential trends to this data reveals different scaling rates, with neutral atoms exhibiting the fastest approximate doubling time at 1.4 years, compared to 2.6 years for superconducting circuits and 5.0 years for ion traps.

Section 2 detailed the remarkable advancements in physical-qubit technologies over the past decades, showcasing multi-order-of-magnitude improvements in coherence times, entanglement fidelity, and achievable system sizes across various platforms. However, as the analysis of entanglement error (Section 2.2.2) illustrates, even state-of-the-art physical qubits possess inherent error rates and face scaling challenges that currently preclude the direct execution of large-scale, fault-tolerant quantum algorithms. The physical error rates, while dramatically reduced over the past decades, remain significantly higher than what complex computations demand, and bridging this fidelity gap is the primary motivation for QEC. Therefore, translating the physical qubit advancements reviewed previously into reliable computational power depends critically on the effective implementation and scaling of QEC protocols. Therefore, we now transition from the physical layer benchmarks to the logical layer, by first delving into the principles of QEC and then surveying the experimental landscape of QEC code implementations designed to protect quantum information and ultimately enable fault-tolerant computation.

### 3 QEC Code Implementation

Inspired by Gottesman’s prioritization of specific QEC codes based on their resource requirements for early fault-tolerance demonstrations [117], numerous experimental efforts have successfully implemented many of these codes, see Table 1. These realizations affirm the viability of using smaller, experimentally accessible codes as the initial steps towards achieving robust, fault-tolerant quantum computation.

**Table 1: Minimum Qubits to demonstrate Fault Tolerance on early implementation** [117]. The 7-qubit code requires 4 ancilla for Error Correction and 1 for testing. We make separate rows for the standard 9-qubit Bacon-Shor code and the two-dimensional (2D) nearest-neighbor (NN) implementation.

Quantum Code Name	Minimum Qubits for Fault Tolerance	Number of Ancilla Qubits
[[4, 2, 2]] code	5	1
[[6, 4, 2]] code	7	1
[[8, 6, 2]] code	9	1
9-qubit Bacon-Shor code	10	1
5-qubit code [118, 119]	11	6
7-qubit code [120]	12	5
Surface code	$\geq 13$	-
2D NN 9-qubit Bacon-Shor code	13	1

Building upon these early demonstrations, this section provides a detailed examination of the broader landscape of experimental QEC code implementations. We will explore the underlying concepts, survey the range of codes and platforms utilized, and analyze key metrics tracking progress towards fault tolerance.

#### 3.1 Concept of QEC

QEC provides a strategy to protect fragile quantum information from noise inherent in physical systems and gate operations. The core principle involves encoding the state of one or more logical qubits into a carefully chosen subspace within a larger Hilbert space spanned by many physical qubits. QEC codes are specifically designed such that common types of physical errors (e.g., single-qubit bit flips or phase flips) map the encoded logical state onto distinguishable, mutually orthogonal error subspaces. This structure enables to extract information about the error that occurred, called error syndrome, through measurements, often involving ancillary qubits. This process reveals the error type and location without directly measuring, and thus collapsing, the encoded logical information itself, allowing for subsequent correction.

The fundamental properties and capabilities of a QEC code are concisely described by the parameters  $[[n, k, d]]$ . Here,  $n$  represents the total number of physical qubits utilized in the code block,  $k$  denotes the number of logical qubits robustly encoded, and  $d$  is the code distance. The distance  $d$  is a crucial metric quantifying the code's error detection and correction power. It corresponds to the minimum number of arbitrary single-qubit errors that could potentially transform one encoded logical state into another, or cause an undetectable error. A code possessing distance  $d$  is guaranteed to detect any combination of up to  $d - 1$  physical errors and correct any combination of up to  $\lfloor(d - 1)/2\rfloor$  physical errors occurring within a code block. Consequently, achieving higher code distances offers enhanced protection against noise, but this typically comes at the cost of requiring a significantly larger number of physical qubits  $n$ .

With the fundamental concepts of encoding, error detection, and code parameters  $[[n, k, d]]$  established, we now survey the key experimental efforts realizing these principles. This review concentrates on the platforms and specific QEC codes where significant progress has been documented in the scientific literature, including both peer-reviewed publications and widely accessible preprints (e.g., via arXiv), providing the basis for the analysis presented in the following sections.

### 3.2 Experiments Considered

Our analysis focuses on the platforms that have demonstrated the most significant experimental progress in multi-qubit operations and the implementation of QEC. These include established approaches like trapped ions [28, 32] and various superconducting circuits [24, 33], alongside rapidly advancing systems such as arrays of neutral atoms held in optical traps [29]. We also consider photonic systems [121], which often leverage different computational models based on linear optics or integrated circuits, and solid-state spin systems like NV centers in diamond [31]. For historical context and early demonstrations, results from Nuclear Magnetic Resonance (NMR) are also included.

The experimental exploration of QEC spans a wide spectrum of codes, reflecting different strategies and complexities. Earliest work often implemented simple Repetition Codes [122] (distance  $d$ , realizing  $[[d, 1, d]]$  parameters for either bit-flip or phase-flip protection) as building blocks or initial demonstrations [11, 123–137]. Significant effort has also focused on early stabilizer codes like the  $[[5, 1, 3]]$  Perfect Code [138–140], as well as various small error detecting codes like the  $[[4, 1, 2]]$  or  $[[4, 2, 2]]$  variants [134, 141–155]. More recent research increasingly targets codes with topological properties or higher potential for fault tolerance, such as Surface Codes [156] implemented with various distances and configurations, often encoding  $k = 1$  [66, 135, 136, 157–161], or  $k = 2$  [66] logical qubits, and Color Codes (e.g.,  $[[7, 1, 3]]$ ,  $[[19, 1, 5]]$ , potentially encoding  $k = 1, 2$ , or even 3 logical qubits) [66, 160, 162–164]. Subsystem codes, notably the Bacon-Shor code [18, 165, 166] (e.g.,  $[[9, 1, 3]]$ ) [155, 167, 168], offer alternative structures for fault tolerance. Additionally, numerous demonstrations use simpler entangled states like Bell states [169–171], primarily for error detection protocols rather than full correction, or employ Cluster States [66], as resources for measurement-based quantum computation which also possess inherent error detection properties. The specific implementations of these codes across the aforementioned platforms form the core dataset analyzed in this section.

Beyond identifying the specific platforms and codes explored, quantifying the progress in QEC experiments requires analyzing dedicated metrics related to these implementations.

### 3.3 Logical Level Metrics

Evaluating the progress in experimental QEC necessitates to track specific metrics that capture the type of code implemented, the hardware platform, the  $[[n, k, d]]$  code parameters, and the achieved performance, often assessed through logical error rates and proximity to fault-tolerance accuracy thresholds. The analysis presented in this section is based on the `qec_exp` dataset, which compiles information on experimental QEC implementations spanning from the earliest demonstrations in 1998 [11] up to recent results in 2024. This dataset covers a diverse range of platforms mentioned above, including superconducting circuits, trapped ions, neutral atoms, NMR systems, and photonic devices.

For each documented implementation, the dataset records key details: the specific QEC code family (e.g., Repetition Code, Surface Code, Color Code), the corresponding publication reference, year of publication, the code's  $[[n, k, d]]$  parameters, and the hardware platform employed. Examining the data chronologically reveals a clear trajectory of progress: beginning with three-qubit repetition codes primarily in NMR systems, the field has advanced significantly to implementing sophisticated codes like surface codes that leverage up to 49 physical qubits on neutral atom arrays and superconducting circuits. Notably, recent milestones captured in the dataset include demonstrations of error correction operating below the fault-tolerance threshold using surface codes [136].

### 3.3.1 Cumulative Growth and Platform Distribution

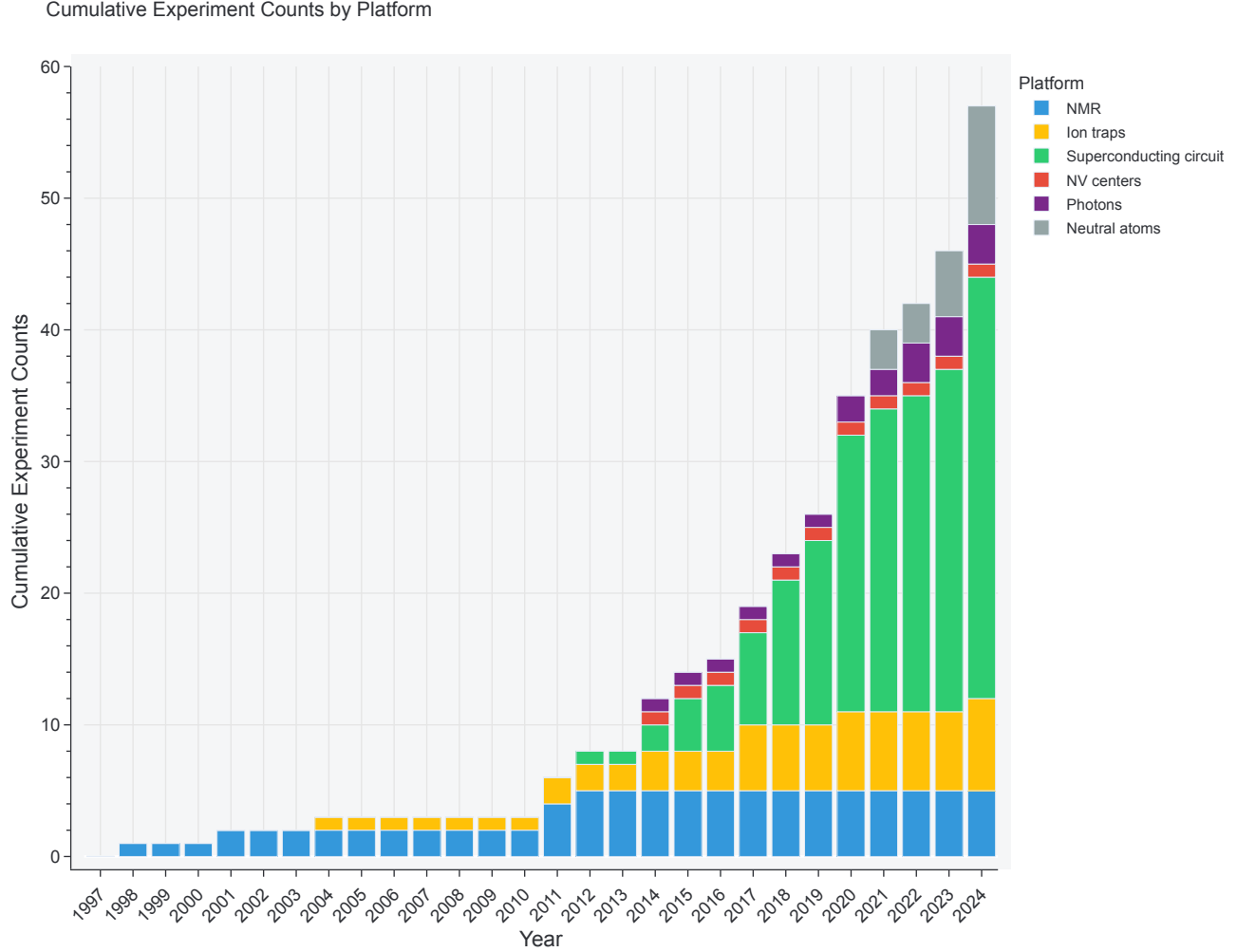


Figure 4: **Cumulative experiment counts by platform.** Total number of published QEC-related experiments up to a given year, categorized by platform. See Section 7.2.1 for a yearly (non cumulative) representation

The field has witnessed substantial growth in experimental QEC activity over the past quarter-century. Figure 4 plots the cumulative count of documented QEC experiments since 1998, broken down by the physical platform employed. The overall trajectory demonstrates significant and accelerating growth in research activity. While NMR platforms hosted the earliest demonstrations, trapped ion systems began contributing consistently around 2004 and show steady growth. Superconducting circuits emerged shortly thereafter and have since become the dominant platform in terms of cumulative experimental output, exhibiting particularly rapid growth in the last decade. Neutral atom platforms represent a more recent but fast-growing contributor to the field, alongside consistent contributions from photonic systems and nascent efforts in NV centers. This cumulative view highlights the increasing investment and progress across multiple hardware modalities in tackling the challenges of QEC. A non-cumulative, year-by-year breakdown is provided in Figure 6 in the Appendices.

### 3.3.2 $[[n, k, d]]$ Representation

As mentioned above, the  $[[n, k, d]]$  parameters provide a concise summary of a QEC code's resource requirements ( $n$ ), encoded information capacity ( $k$ ), and error correction strength ( $d$ ). Figure 5 visualizes the landscape of experimentally realized QEC codes by plotting the number of physical qubits ( $n$ ) against the achieved code distance ( $d$ ). Each point represents a documented experiment, labeled by the code type and the number of logical qubits encoded ( $k$ ).

### Aggregated Quantum Error Correction Parameters

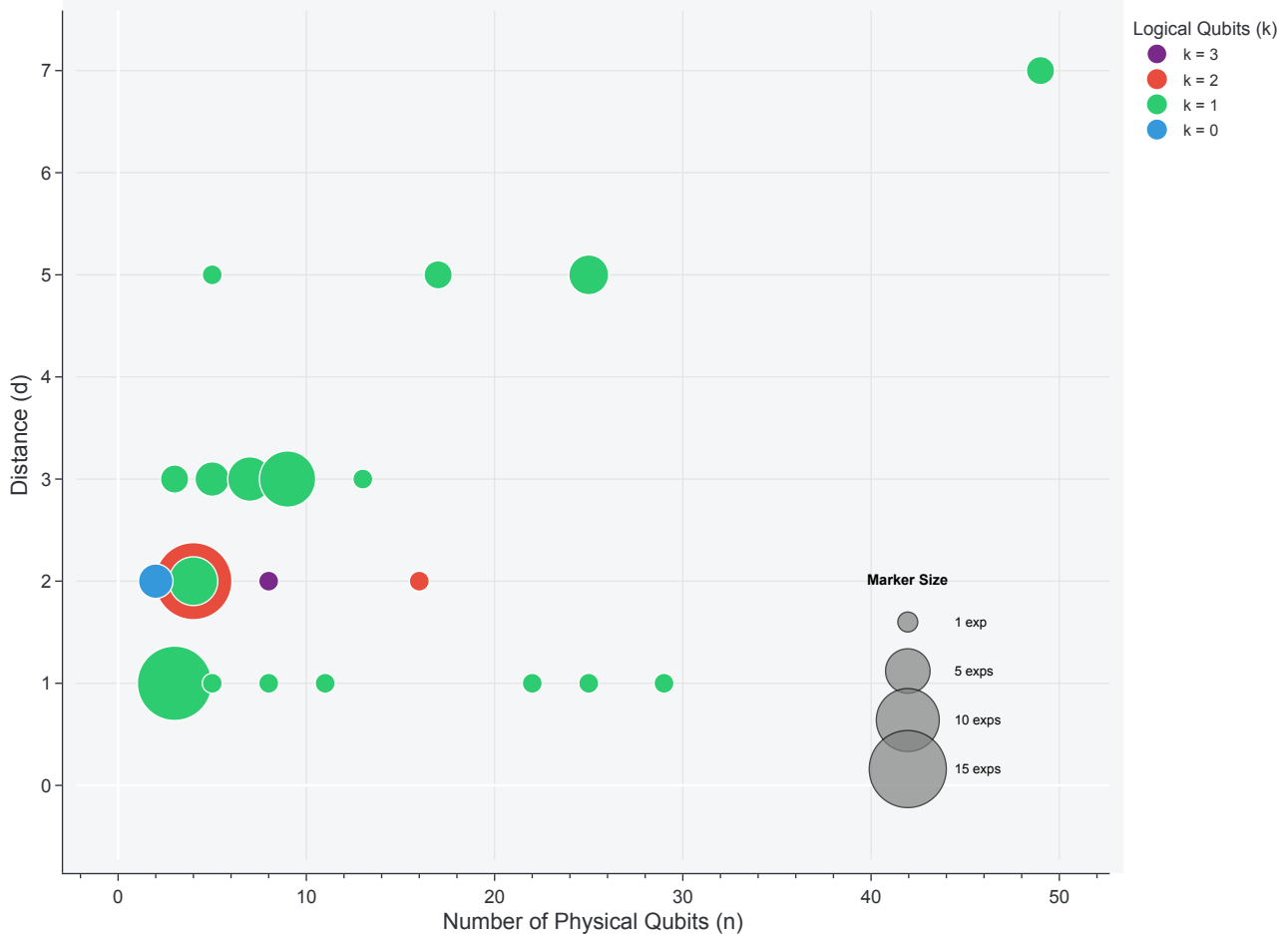


Figure 5: **QEC Code Parameters**  $[[n, k, d]]$ . Scatter plot showing the number of physical qubits ( $n$ ) versus the code distance ( $d$ ) for experimentally implemented QEC codes. Points are labeled by the code type and logical qubit count ( $k$ ). We see the horizontal line at  $d = 1$  corresponding to the classical repetition code and the square root profile of the surface code where  $d \propto \sqrt{n}$ . Realized codes focus on encoding a single logical qubit ( $k = 1$ ), even though implementations with more logical qubits do exist.

The plot reveals that a significant portion of experimental work has focused on codes with relatively low distance ( $d \leq 3$ ) and using fewer than 50 physical qubits. These implementations often serve as crucial demonstrations of QEC principles, stabilizer measurements, or specific code components. Notably, simple repetition codes ( $k = 1$ , various  $d$ ) and early stabilizer codes like the  $[[5, 1, 3]]$  code are represented in this region. However, the figure also clearly illustrates the ongoing effort to push towards higher code distances, which offer protection against a greater number of physical errors, which is a prerequisite for fault tolerance. Milestones include implementations of surface codes and color codes reaching  $d = 3$ ,  $d = 5$  and even  $d = 7$ , requiring substantially more physical qubits (approaching  $n = 50$  for  $d = 7$ ).

#### 3.3.3 QEC Performance Benchmarks

While Section 3.3 introduces logical level metrics such as the cumulative count of experiments and the  $[[n, k, d]]$  parameters realized, a dedicated analysis of the performance of implemented QEC codes is essential for benchmarking progress towards fault tolerance. Key performance indicators include the suppression of logical errors relative to physical errors, often quantified by the suppression factor  $\Lambda$ , demonstrations of logical qubit lifetime extension beyond the physical qubit limit (break-even), and operation below theoretical fault-tolerance thresholds. Recent experiments

have made significant strides in these areas. For instance, logical error suppression when increasing code distance has been quantified, scaling from distance-3 to distance-5, suppression factors of approximately 2.15(2), 1.69(6), and 1.56(2) were measured for different dynamic surface code implementations [161], and a factor of  $\Lambda = 1.56(4)$  was observed for the color code, which simulations indicated was below threshold [163]. While an earlier surface code experiment showed only modest improvement between distance-3 and distance-5 logical qubits (logical error per cycle of 2.914% vs 3.028%) [135], the following demonstration achieved significant suppression ( $\Lambda = 2.14 \pm 0.02$ ) when scaling from distance-5 to distance-7 [136]. This latter work also reported operating both distance-5 and distance-7 surface codes below the fault-tolerance threshold, achieving a logical error rate per cycle of  $0.143\% \pm 0.003\%$  for the 101-qubit distance-7 code [136]. Furthermore, this distance-7 logical memory surpassed the break-even point, exhibiting a lifetime  $2.4 \pm 0.3$  times longer than its best constituent physical qubit [136]. Although these recent achievements mark critical milestones, the overall number of such demonstrations remains insufficient to establish statistically significant trends in logical error suppression or performance scaling across different codes and platforms at this time.

## 4 Conclusion

In this work, we have introduced an online and open-source tool [26] to track the progress of several chosen metrics in the quantum computing stack, from low-level characteristics like relaxation and coherence times to higher-level ones like QEC code parameters.

Our analysis reveals remarkable advances: physical-qubit coherence and gate fidelity have improved by orders of magnitude, while processor scale has grown exponentially, enabling access to hundreds and even thousands of qubits [68, 112]. Concurrently, experimental QEC has progressed from foundational demonstrations [11, 123] to implementing sophisticated codes like surface and color codes with increasing scale  $n$  and distance  $d$  across multiple leading platforms [136, 159, 160].

Despite the impressive progress, achieving robust fault-tolerant quantum computation requires overcoming persistent critical challenges. Three key obstacles include: (1) The resource overhead problem: QEC requires encoding information across multiple physical qubits, dramatically increasing hardware complexity. For instance, factorizing a 2048-bit RSA integer using Shor's algorithm would require approximately one million superconducting qubits despite only needing 1,537 algorithmic qubits, with each algorithmic qubit requiring at most 1,352 physical qubits for noise suppression ( $d = 25$ ) [7], (2) The processing of encoded information: Logical gates must operate directly on encoded qubits without decoding, requiring complex physical operations where a single logical two-qubit gate can involve thousands of state preparations and physical gate operations. Achieving universal gate sets adds further overhead through magic state distillation [172] or cultivation [173], which can consume a significant fraction of logical qubits [154, 163, 164], and (3) The decoding problem: Decoders must process error syndrome data at quantum computer clock speeds, potentially handling gigabit-per-second data rates per logical qubit, requiring scalable decoding algorithms that balance accuracy, latency, and scalability for these thousands of logical qubits involved.

While long  $T_1$  and  $T_2$  times are essential for preserving quantum information, the comparison with gate and QEC cycle times ultimately determines how many operations can be performed before quantum information is lost. Future work will thus focus on incorporating finer-grained metrics essential for fault-tolerance such as the QEC cycle time but also logical qubit performance under repeated correction cycles, logical error suppression factors  $\Lambda$ , post-selection rates, detailed ancilla qubit counts, logical qubit half-lives, alongside benchmarks for key subroutines including magic state distillation [154, 163, 164] and GHZ state preparation [155, 160, 174–177]. Synthesizing multi-layered progress, facilitated by the presented resource, is vital for navigating this rapidly evolving field towards the ultimate goal of impactful fault-tolerant quantum computation.

Designed for flexibility and community contribution, our tool provides a unified resource that will be developed as the field continues to grow. We hope it proves valuable for physicists and QEC researchers by having all the resources in one place to make fair comparisons between technologies.

## 5 Acknowledgements

We thank Pascal Scholl and Antoine Browaeys for insightful discussions during the preparation of this manuscript. We thank Julius de Hond and Louis Vignoli for reading a draft of this paper and providing useful feedback. We

thank the Pasqal team, and in particular Lucas Lassablière and Adrien Signoles, for cultivating an environment that enabled this work.

## 6 References

### References

- [1] Seth Lloyd. Universal Quantum Simulators. *Science*, 273(5278):1073–1078, August 1996. doi: 10.1126/science.273.5278.1073.
- [2] Peter W. Shor. Polynomial-Time Algorithms for Prime Factorization and Discrete Logarithms on a Quantum Computer. *SIAM Journal on Computing*, 26(5):1484–1509, October 1997. ISSN 0097-5397, 1095-7111. doi: 10.1137/S0097539795293172.
- [3] Edward Farhi, Jeffrey Goldstone, Sam Gutmann, Joshua Lapan, Andrew Lundgren, and Daniel Predu. A Quantum Adiabatic Evolution Algorithm Applied to Random Instances of an NP-Complete Problem. *Science*, 292(5516):472–475, April 2001. ISSN 0036-8075, 1095-9203. doi: 10.1126/science.1057726.
- [4] Alán Aspuru-Guzik, Anthony D. Dutoi, Peter J. Love, and Martin Head-Gordon. Simulated Quantum Computation of Molecular Energies. *Science*, 309(5741):1704–1707, September 2005. ISSN 0036-8075, 1095-9203. doi: 10.1126/science.1113479.
- [5] Craig Gidney and Martin Ekerå. How to factor 2048 bit RSA integers in 8 hours using 20 million noisy qubits. *Quantum*, 5:433, April 2021. ISSN 2521-327X. doi: 10.22331/q-2021-04-15-433.
- [6] Sivaprasad Omanakuttan, Zichang He, Zhiwei Zhang, Tianyi Hao, Arman Babakhani, Sami Boulebnane, Shouvanik Chakrabarti, Dylan Herman, Joseph Sullivan, Michael A. Perlin, Ruslan Shaydulin, and Marco Pistoia. Threshold for Fault-tolerant Quantum Advantage with the Quantum Approximate Optimization Algorithm. April 2025. doi: 10.48550/arXiv.2504.01897.
- [7] Craig Gidney. How to factor 2048 bit RSA integers with less than a million noisy qubits. May 2025. doi: 10.48550/arXiv.2505.15917.
- [8] Hengyun Zhou, Casey Duckering, Chen Zhao, Dolev Bluvstein, Madelyn Cain, Aleksander Kubica, Sheng-Tao Wang, and Mikhail D. Lukin. Resource Analysis of Low-Overhead Transversal Architectures for Reconfigurable Atom Arrays. May 2025. doi: 10.48550/arXiv.2505.15907.
- [9] Ian D. Kivlichan, Craig Gidney, Dominic W. Berry, Nathan Wiebe, Jarrod McClean, Wei Sun, Zhang Jiang, Nicholas Rubin, Austin Fowler, Alán Aspuru-Guzik, Hartmut Neven, and Ryan Babbush. Improved Fault-Tolerant Quantum Simulation of Condensed-Phase Correlated Electrons via Trotterization. *Quantum*, 4:296, July 2020. ISSN 2521-327X. doi: 10.22331/q-2020-07-16-296.
- [10] Earl T. Campbell. Early fault-tolerant simulations of the Hubbard model. *Quantum Science and Technology*, 7(1):015007, January 2022. ISSN 2058-9565. doi: 10.1088/2058-9565/ac3110.
- [11] D. G. Cory, M. D. Price, W. Maas, E. Knill, R. Laflamme, W. H. Zurek, T. F. Havel, and S. S. Somaroo. Experimental Quantum Error Correction. *Phys. Rev. Lett.*, 81(10):2152–2155, September 1998. doi: 10.1103/PhysRevLett.81.2152.
- [12] Q. A. Turchette, C. S. Wood, B. E. King, C. J. Myatt, D. Leibfried, W. M. Itano, C. Monroe, and D. J. Wineland. Deterministic entanglement of two trapped ions. *Physical Review Letters*, 81(17):3631–3634, October 1998. ISSN 0031-9007, 1079-7114. doi: 10.1103/PhysRevLett.81.3631.
- [13] Y. Nakamura, Yu A. Pashkin, and J. S. Tsai. Coherent control of macroscopic quantum states in a single-Cooper-pair box. *Nature*, 398(6730):786–788, April 1999. ISSN 0028-0836, 1476-4687. doi: 10.1038/19718.
- [14] P.W. Shor. Fault-tolerant quantum computation. In *Proceedings of 37th Conference on Foundations of Computer Science*, pages 56–65, October 1996. doi: 10.1109/SFCS.1996.548464.
- [15] Isaac H. Kim, Eunseok Lee, Ye-Hua Liu, Sam Pallister, William Pol, and Sam Roberts. Fault-tolerant resource estimate for quantum chemical simulations: Case study on Li-ion battery electrolyte molecules. *Physical Review Research*, 4(2):023019, April 2022. ISSN 2643-1564. doi: 10.1103/PhysRevResearch.4.023019.

- [16] Andrew Steane. Multiple Particle Interference and Quantum Error Correction. *Proceedings of the Royal Society of London. Series A: Mathematical, Physical and Engineering Sciences*, 452(1954):2551–2577, November 1996. ISSN 1364-5021, 1471-2946. doi: 10.1098/rspa.1996.0136.
- [17] Eric Dennis, Alexei Kitaev, Andrew Landahl, and John Preskill. Topological quantum memory. *Journal of Mathematical Physics*, 43(9):4452–4505, September 2002. ISSN 0022-2488, 1089-7658. doi: 10.1063/1.1499754.
- [18] Peter W. Shor. Scheme for reducing decoherence in quantum computer memory. *Physical Review A*, 52(4): R2493–R2496, October 1995. doi: 10.1103/PhysRevA.52.R2493.
- [19] A. M. Steane. Simple quantum error-correcting codes. *Physical Review A*, 54(6):4741–4751, December 1996. doi: 10.1103/PhysRevA.54.4741.
- [20] Daniel Eric Gottesman. *Stabilizer Codes and Quantum Error Correction*. PhD thesis, California Institute of Technology, 1997.
- [21] Emanuel Knill and Raymond Laflamme. Theory of quantum error-correcting codes. *Physical Review A*, 55(2): 900–911, February 1997. doi: 10.1103/PhysRevA.55.900.
- [22] John Preskill. Fault-tolerant quantum computation. December 1997. doi: 10.48550/arXiv.quant-ph/9712048.
- [23] Emanuel Knill, Raymond Laflamme, and Wojciech H. Zurek. Resilient Quantum Computation. *Science*, 279 (5349):342–345, January 1998. doi: 10.1126/science.279.5349.342.
- [24] Morten Kjaergaard, Mollie E. Schwartz, Jochen Braumüller, Philip Krantz, Joel I.-Jan Wang, Simon Gustavsson, and William D. Oliver. Superconducting Qubits: Current State of Play. *Annual Review of Condensed Matter Physics*, 11(1):369–395, March 2020. ISSN 1947-5454, 1947-5462. doi: 10.1146/annurev-conmatphys-031119-050605.
- [25] Victor V. Albert and Philippe Faist. Quantum Realizations The Error Correction Zoo. [https://errorcorrectionzoo.org/list/quantum\\_realizations](https://errorcorrectionzoo.org/list/quantum_realizations), 2025.
- [26] Francois-Marie Le Régent. Awesome Quantum Computing Experiments. <https://github.com/francois-marie/awesome-quantum-computing-experiments>, April 2025.
- [27] M.A. Nielsen and I. L. Chuang. *Quantum Computation and Quantum Information 10th Anniversary Edition*. Cambridge University Press, 2000. doi: 10.1017/CBO9780511976667.
- [28] Colin D. Bruzewicz, John Chiaverini, Robert McConnell, and Jeremy M. Sage. Trapped-Ion Quantum Computing: Progress and Challenges. *Applied Physics Reviews*, 6(2):021314, June 2019. ISSN 1931-9401. doi: 10.1063/1.5088164.
- [29] Karen Wintersperger, Florian Dommert, Thomas Ehmer, Andrey Hoursanov, Johannes Klepsch, Wolfgang Mauerer, Georg Reuber, Thomas Strohm, Ming Yin, and Sebastian Luber. Neutral Atom Quantum Computing Hardware: Performance and End-User Perspective. *EPJ Quantum Technology*, 10(1):32, December 2023. ISSN 2662-4400, 2196-0763. doi: 10.1140/epjqt/s40507-023-00190-1.
- [30] Arne Laucht, Frank Hohls, Niels Ubbelohde, M Fernando Gonzalez-Zalba, David J Reilly, Søren Stobbe, Tim Schröder, Pasquale Scarlino, Jonne V Koski, Andrew Dzurak, Chih-Hwan Yang, Jun Yoneda, Ferdinand Kuemmeth, Hendrik Bluhm, Jarryd Pla, Charles Hill, Joe Salfi, Akira Oiwa, Juha T Muhonen, Ewold Verhagen, M D LaHaye, Hyun Ho Kim, Adam W Tsien, Dimitrie Culcer, Attila Geresdi, Jan A Mol, Varun Mohan, Prashant K Jain, and Jonathan Baugh. Roadmap on quantum nanotechnologies. *Nanotechnology*, 32(16): 162003, February 2021. ISSN 0957-4484. doi: 10.1088/1361-6528/abb333.
- [31] Sébastien Pezzagna and Jan Meijer. Quantum computer based on color centers in diamond. *Applied Physics Reviews*, 8(1):011308, February 2021. ISSN 1931-9401. doi: 10.1063/5.0007444.
- [32] Kenneth R. Brown, John Chiaverini, Jeremy M. Sage, and Hartmut Häffner. Materials challenges for trapped-ion quantum computers. *Nature Reviews Materials*, 6(10):892–905, October 2021. ISSN 2058-8437. doi: 10.1038/s41578-021-00292-1.
- [33] Atharv Joshi, Kyungjoo Noh, and Yvonne Y. Gao. Quantum information processing with bosonic qubits in circuit QED. *Quantum Science and Technology*, 6(3):033001, April 2021. doi: 10.1088/2058-9565/abe989.

- [34] Y. Nakamura, Yu. A. Pashkin, T. Yamamoto, and J. S. Tsai. Charge Echo in a Cooper-Pair Box. *Physical Review Letters*, 88(4):047901, January 2002. doi: 10.1103/PhysRevLett.88.047901.
- [35] D. Vion, A. Aassime, A. Cottet, P. Joyez, H. Pothier, C. Urbina, D. Esteve, and M. H. Devoret. Manipulating the Quantum State of an Electrical Circuit. *Science*, 296(5569):886–889, May 2002. ISSN 0036-8075, 1095-9203. doi: 10.1126/science.1069372.
- [36] I. Chiorescu, Y. Nakamura, C. J. P. M. Harmans, and J. E. Mooij. Coherent Quantum Dynamics of a Superconducting Flux Qubit. *Science*, 299(5614):1869–1871, March 2003. ISSN 0036-8075, 1095-9203. doi: 10.1126/science.1081045.
- [37] P. Bertet, I. Chiorescu, G. Burkard, K. Semba, C. J. P. M. Harmans, D. P. DiVincenzo, and J. E. Mooij. Dephasing of a superconducting qubit induced by photon noise. *Physical Review Letters*, 95(25):257002, December 2005. ISSN 0031-9007, 1079-7114. doi: 10.1103/PhysRevLett.95.257002.
- [38] A. A. Houck, J. A. Schreier, B. R. Johnson, J. M. Chow, Jens Koch, J. M. Gambetta, D. I. Schuster, L. Frunzio, M. H. Devoret, S. M. Girvin, and R. J. Schoelkopf. Controlling the spontaneous emission of a superconducting transmon qubit. *Physical Review Letters*, 101(8):080502, August 2008. ISSN 0031-9007, 1079-7114. doi: 10.1103/PhysRevLett.101.080502.
- [39] H. Wang, M. Hofheinz, M. Ansmann, R. C. Bialczak, E. Lucero, M. Neeley, A. D. O’Connell, D. Sank, J. Wenner, A. N. Cleland, and John M. Martinis. Measurement of the Decay of Fock States in a Superconducting Quantum Circuit. *Physical Review Letters*, 101(24):240401, December 2008. doi: 10.1103/PhysRevLett.101.240401.
- [40] Vladimir E. Manucharyan, Jens Koch, Leonid Glazman, and Michel Devoret. Fluxonium: Single Cooper pair circuit free of charge offsets. *Science*, 326(5949):113–116, October 2009. ISSN 0036-8075, 1095-9203. doi: 10.1126/science.1175552.
- [41] Jonas Bylander, Simon Gustavsson, Fei Yan, Fumiki Yoshihara, Khalil Harrabi, George Fitch, David G. Cory, Yasunobu Nakamura, Jaw-Shen Tsai, and William D. Oliver. Dynamical decoupling and noise spectroscopy with a superconducting flux qubit. *Nature Physics*, 7(7):565–570, July 2011. ISSN 1745-2473, 1745-2481. doi: 10.1038/nphys1994.
- [42] Hanhee Paik, D. I. Schuster, Lev S. Bishop, G. Kirchmair, G. Catelani, A. P. Sears, B. R. Johnson, M. J. Reagor, L. Frunzio, L. I. Glazman, S. M. Girvin, M. H. Devoret, and R. J. Schoelkopf. Observation of High Coherence in Josephson Junction Qubits Measured in a Three-Dimensional Circuit QED Architecture. *Physical Review Letters*, 107(24):240501, December 2011. ISSN 0031-9007, 1079-7114. doi: 10.1103/PhysRevLett.107.240501.
- [43] Chad Rigetti, Stefano Poletto, Jay M. Gambetta, B. L. T. Plourde, Jerry M. Chow, A. D. Corcoles, John A. Smolin, Seth T. Merkel, J. R. Rozen, George A. Keefe, Mary B. Rothwell, Mark B. Ketchen, and M. Steffen. Superconducting qubit in waveguide cavity with coherence time approaching 0.1ms. *Physical Review B*, 86(10):100506, September 2012. ISSN 1098-0121, 1550-235X. doi: 10.1103/PhysRevB.86.100506.
- [44] J. Chang, M. R. Vissers, A. D. Corcoles, M. Sandberg, J. Gao, David W. Abraham, Jerry M. Chow, Jay M. Gambetta, M. B. Rothwell, G. A. Keefe, Matthias Steffen, and D. P. Pappas. Improved superconducting qubit coherence using titanium nitride. *Applied Physics Letters*, 103(1):012602, July 2013. ISSN 0003-6951, 1077-3118. doi: 10.1063/1.4813269.
- [45] Ioan M. Pop, Kurtis Geerlings, Gianluigi Catelani, Robert J. Schoelkopf, Leonid I. Glazman, and Michel H. Devoret. Coherent suppression of electromagnetic dissipation due to superconducting quasiparticles. *Nature*, 508(7496):369–372, April 2014. ISSN 1476-4687. doi: 10.1038/nature13017.
- [46] X. Y. Jin, A. Kamal, A. P. Sears, T. Gudmundsen, D. Hover, J. Miloxi, R. Slattery, F. Yan, J. Yoder, T. P. Orlando, S. Gustavsson, and W. D. Oliver. Thermal and Residual Excited-State Population in a 3D Transmon Qubit. *Physical Review Letters*, 114(24):240501, June 2015. ISSN 0031-9007, 1079-7114. doi: 10.1103/PhysRevLett.114.240501.
- [47] Nissim Ofek, Andrei Petrenko, Reinier Heeres, Philip Reinhold, Zaki Leghtas, Brian Vlastakis, Yehan Liu, Luigi Frunzio, S. M. Girvin, L. Jiang, Mazyar Mirrahimi, M. H. Devoret, and R. J. Schoelkopf. Extending the lifetime of a quantum bit with error correction in superconducting circuits. *Nature*, 536(7617):441–445, August 2016. ISSN 1476-4687. doi: 10.1038/nature18949.

- [48] Chen Wang, Yvonne Y. Gao, Philip Reinhold, R. W. Heeres, Nissim Ofek, Kevin Chou, Christopher Axline, Matthew Reagor, Jacob Blumoff, K. M. Sliwa, L. Frunzio, S. M. Girvin, Liang Jiang, M. Mirrahimi, M. H. Devoret, and R. J. Schoelkopf. A Schrodinger Cat Living in Two Boxes. *Science*, 352(6289):1087–1091, May 2016. ISSN 0036-8075, 1095-9203. doi: 10.1126/science.aaf2941.
- [49] F. Yan, S. Gustavsson, A. Kamal, J. Birenbaum, A. P. Sears, D. Hover, D. Rosenberg, G. Samach, T. J. Gudmundsen, J. L. Yoder, T. P. Orlando, J. Clarke, A. J. Kerman, and W. D. Oliver. The Flux Qubit Revisited to Enhance Coherence and Reproducibility. *Nature Communications*, 7(1):12964, November 2016. ISSN 2041-1723. doi: 10.1038/ncomms12964.
- [50] S. Rosenblum, P. Reinhold, M. Mirrahimi, Liang Jiang, L. Frunzio, and R. J. Schoelkopf. Fault-tolerant detection of a quantum error. *Science*, 361(6399):266–270, July 2018. ISSN 0036-8075, 1095-9203. doi: 10.1126/science.aat3996.
- [51] Ling Hu, Yuwei Ma, Weizhou Cai, Xianghao Mu, Yuan Xu, Weiting Wang, Yukai Wu, Haiyan Wang, Yipu Song, Changling Zou, S. M. Girvin, L.-M. Duan, and Luyan Sun. Demonstration of quantum error correction and universal gate set on a binomial bosonic logical qubit. *Nature Physics*, 15(5):503–508, May 2019. ISSN 1745-2473, 1745-2481. doi: 10.1038/s41567-018-0414-3.
- [52] Long B. Nguyen, Yen-Hsiang Lin, Aaron Somoroff, Raymond Mencia, Nicholas Grabon, and Vladimir E. Manucharyan. The high-coherence fluxonium qubit. *Physical Review X*, 9(4):041041, November 2019. ISSN 2160-3308. doi: 10.1103/PhysRevX.9.041041.
- [53] Raphaël Lescanne, Marius Villiers, Théau Peronnin, Alain Sarlette, Matthieu Delbecq, Benjamin Huard, Takis Kontos, Mazyar Mirrahimi, and Zaki Leghtas. Exponential suppression of bit-flips in a qubit encoded in an oscillator. *Nature Physics*, 16(5):509–513, March 2020. ISSN 1745-2481. doi: 10.1038/s41567-020-0824-x.
- [54] C. Berdou, A. Murani, U. Réglade, W.C. Smith, M. Villiers, J. Palomo, M. Rosticher, A. Denis, P. Morfin, M. Delbecq, T. Kontos, N. Pankratova, F. Rautschke, T. Peronnin, L.-A. Sellem, P. Rouchon, A. Sarlette, M. Mirrahimi, P. Campagne-Ibarcq, S. Jezouin, R. Lescanne, and Z. Leghtas. One Hundred Second Bit-Flip Time in a Two-Photon Dissipative Oscillator. *PRX Quantum*, 4(2), June 2023. ISSN 2691-3399. doi: 10.1103/prxquantum.4.020350.
- [55] Antoine Marquet, Antoine Essig, Joachim Cohen, Nathanaël Cottet, Anil Murani, Emanuele Albertinale, Simon Dupouy, Audrey Bienfait, Théau Peronnin, Sébastien Jezouin, Raphaël Lescanne, and Benjamin Huard. Autoparametric resonance extending the bit-flip time of a cat qubit up to 0.3 s. *Physical Review X*, 14(2): 021019, April 2024. ISSN 2160-3308. doi: 10.1103/PhysRevX.14.021019.
- [56] Ulysse Réglade, Adrien Bocquet, Ronan Gautier, Joachim Cohen, Antoine Marquet, Emanuele Albertinale, Natalia Pankratova, Mattis Hallén, Felix Rautschke, Lev-Arcady Sellem, Pierre Rouchon, Alain Sarlette, Mazyar Mirrahimi, Philippe Campagne-Ibarcq, Raphaël Lescanne, Sébastien Jezouin, and Zaki Leghtas. Quantum control of a cat-qubit with bit-flip times exceeding ten seconds. *Nature*, 629(8013):778–783, May 2024. ISSN 0028-0836, 1476-4687. doi: 10.1038/s41586-024-07294-3.
- [57] T. W. Larsen, K. D. Petersson, F. Kuemmeth, T. S. Jespersen, P. Krogstrup, J. Nygård, and C. M. Marcus. A Semiconductor Nanowire-Based Superconducting Qubit. *Physical Review Letters*, 115(12):127001, September 2015. ISSN 0031-9007, 1079-7114. doi: 10.1103/PhysRevLett.115.127001.
- [58] L. Casparis, T. W. Larsen, M. S. Olsen, F. Kuemmeth, P. Krogstrup, J. Nygård, K. D. Petersson, and C. M. Marcus. Gatemon Benchmarking and Two-Qubit Operation. *Physical Review Letters*, 116(15):150505, April 2016. ISSN 0031-9007, 1079-7114. doi: 10.1103/PhysRevLett.116.150505.
- [59] F. Luthi, T. Stavenga, O. W. Enzing, A. Bruno, C. Dickel, N. K. Langford, M. A. Rol, T. S. Jespersen, J. Nygård, P. Krogstrup, and L. DiCarlo. Evolution of Nanowire Transmons and Their Quantum Coherence in Magnetic Field. *Physical Review Letters*, 120(10):100502, March 2018. ISSN 0031-9007, 1079-7114. doi: 10.1103/PhysRevLett.120.100502.
- [60] C. Langer, R. Ozeri, J. D. Jost, J. Chiaverini, B. DeMarco, A. Ben-Kish, R. B. Blakestad, J. Britton, D. B. Hume, W. M. Itano, D. Leibfried, R. Reichle, T. Rosenband, T. Schaetz, P. O. Schmidt, and D. J. Wineland. Long-Lived Qubit Memory Using Atomic Ions. *Physical Review Letters*, 95(6):060502, August 2005. doi: 10.1103/PhysRevLett.95.060502.

- [61] T. P. Harty, D. T. C. Allcock, C. J. Ballance, L. Guidoni, H. A. Janacek, N. M. Linke, D. N. Stacey, and D. M. Lucas. High-Fidelity Preparation, Gates, Memory, and Readout of a Trapped-Ion Quantum Bit. *Physical Review Letters*, 113(22):220501, November 2014. doi: 10.1103/PhysRevLett.113.220501.
- [62] Ye Wang, Mark Um, Junhua Zhang, Shuoming An, Ming Lyu, Jing-Ning Zhang, L.-M. Duan, Dahyun Yum, and Kihwan Kim. Single-qubit quantum memory exceeding ten-minute coherence time. *Nature Photonics*, 11(10):646–650, October 2017. ISSN 1749-4893. doi: 10.1038/s41566-017-0007-1.
- [63] Pengfei Wang, Chun-Yang Luan, Mu Qiao, Mark Um, Junhua Zhang, Ye Wang, Xiao Yuan, Mile Gu, Jingning Zhang, and Kihwan Kim. Single ion qubit with estimated coherence time exceeding one hour. *Nature Communications*, 12(1):233, January 2021. ISSN 2041-1723. doi: 10.1038/s41467-020-20330-w.
- [64] Matthew P. A. Jones, Jerome Beugnon, Alpha Gaëtan, Junxiang Zhang, Gaetan Messin, Antoine Browaeys, and Philippe Grangier. Fast Quantum State Control of a Single Trapped Neutral Atom. *Physical Review A*, 75(4):040301, April 2007. ISSN 1050-2947, 1094-1622. doi: 10.1103/PhysRevA.75.040301.
- [65] Jacob P. Covey, Ivaylo S. Madjarov, Alexandre Cooper, and Manuel Endres. 2000-Times Repeated Imaging of Strontium Atoms in Clock-Magic Tweezer Arrays. *Physical Review Letters*, 122(17):173201, May 2019. doi: 10.1103/PhysRevLett.122.173201.
- [66] Dolev Bluvstein, Harry Levine, Giulia Semeghini, Tout T. Wang, Sepehr Ebadi, Marcin Kalinowski, Alexander Keesling, Nishad Maskara, Hannes Pichler, Markus Greiner, Vladan Vuletić, and Mikhail D. Lukin. A quantum processor based on coherent transport of entangled atom arrays. *Nature*, 604(7906):451–456, April 2022. ISSN 0028-0836, 1476-4687. doi: 10.1038/s41586-022-04592-6.
- [67] T. M. Graham, Y. Song, J. Scott, C. Poole, L. Phuttitarn, K. Jooya, P. Eichler, X. Jiang, A. Marra, B. Grinkemeyer, M. Kwon, M. Ebert, J. Cherek, M. T. Lichtman, M. Gillette, J. Gilbert, D. Bowman, T. Ballance, C. Campbell, E. D. Dahl, O. Crawford, N. S. Blunt, B. Rogers, T. Noel, and M. Saffman. Demonstration of multi-qubit entanglement and algorithms on a programmable neutral atom quantum computer. *Nature*, 604(7906):457–462, April 2022. ISSN 0028-0836, 1476-4687. doi: 10.1038/s41586-022-04603-6.
- [68] Hannah J. Manetsch, Gyohei Nomura, Elie Bataille, Kon H. Leung, Xudong Lv, and Manuel Endres. A tweezer array with 6100 highly coherent atomic qubits. December 2024. doi: 10.48550/arXiv.2403.12021.
- [69] Joel I.-Jan Wang, Daniel Rodan-Legrain, Landry Bretheau, Daniel L. Campbell, Bharath Kannan, David Kim, Morten Kjaergaard, Philip Krantz, Gabriel O. Samach, Fei Yan, Jonilyn L. Yoder, Kenji Watanabe, Takashi Taniguchi, Terry P. Orlando, Simon Gustavsson, Pablo Jarillo-Herrero, and William D. Oliver. Quantum coherent control of a hybrid superconducting circuit made with graphene-based van der Waals heterostructures. *Nature Nanotechnology*, 14(2):120–125, February 2019. ISSN 1748-3387, 1748-3395. doi: 10.1038/s41565-018-0329-2.
- [70] Matthias Steffen, M. Ansmann, Radoslaw C. Bialczak, N. Katz, Erik Lucero, R. McDermott, Matthew Neeley, E. M. Weig, A. N. Cleland, and John M. Martinis. Measurement of the Entanglement of Two Superconducting Qubits via State Tomography. *Science*, 313(5792):1423–1425, September 2006. doi: 10.1126/science.1130886.
- [71] L. DiCarlo, J. M. Chow, J. M. Gambetta, Lev S. Bishop, B. R. Johnson, D. I. Schuster, J. Majer, A. Blais, L. Frunzio, S. M. Girvin, and R. J. Schoelkopf. Demonstration of Two-Qubit Algorithms with a Superconducting Quantum Processor. *Nature*, 460(7252):240–244, July 2009. ISSN 0028-0836, 1476-4687. doi: 10.1038/nature08121.
- [72] Jerry M. Chow, Jay M. Gambetta, A. D. Corcoles, Seth T. Merkel, John A. Smolin, Chad Rigetti, S. Poletto, George A. Keefe, Mary B. Rothwell, J. R. Rozen, Mark B. Ketchen, and M. Steffen. Complete universal quantum gate set approaching fault-tolerant thresholds with superconducting qubits. *Physical Review Letters*, 109(6):060501, August 2012. ISSN 0031-9007, 1079-7114. doi: 10.1103/PhysRevLett.109.060501.
- [73] R. Barends, J. Kelly, A. Megrant, A. Veitia, D. Sank, E. Jeffrey, T. C. White, J. Mutus, A. G. Fowler, B. Campbell, Y. Chen, Z. Chen, B. Chiaro, A. Dunsworth, C. Neill, P. O’Malley, P. Roushan, A. Vainsencher, J. Wenner, A. N. Korotkov, A. N. Cleland, and John M. Martinis. Logic gates at the surface code threshold: Superconducting qubits poised for fault-tolerant quantum computing. *Nature*, 508(7497):500–503, April 2014. ISSN 0028-0836, 1476-4687. doi: 10.1038/nature13171.
- [74] Sarah Sheldon, Easwar Magesan, Jerry M. Chow, and Jay M. Gambetta. Procedure for systematically tuning

- up crosstalk in the cross resonance gate. *Physical Review A*, 93(6):060302, June 2016. ISSN 2469-9926, 2469-9934. doi: 10.1103/PhysRevA.93.060302.
- [75] M. Kjaergaard, M. E. Schwartz, A. Greene, G. O. Samach, A. Bengtsson, M. O’Keeffe, C. M. McNally, J. Braumüller, D. K. Kim, P. Krantz, M. Marvian, A. Melville, B. M. Niedzielski, Y. Sung, R. Winik, J. Yoder, D. Rosenberg, K. Obenland, S. Lloyd, T. P. Orlando, I. Marvian, S. Gustavsson, and W. D. Oliver. Demonstration of Density Matrix Exponentiation Using a Superconducting Quantum Processor. *Physical Review X*, 12(1):011005, January 2022. doi: 10.1103/PhysRevX.12.011005.
- [76] L. Isenhower, E. Urban, X. L. Zhang, A. T. Gill, T. Henage, T. A. Johnson, T. G. Walker, and M. Saffman. Demonstration of a neutral atom controlled-NOT quantum gate. *Physical Review Letters*, 104(1):010503, January 2010. ISSN 0031-9007, 1079-7114. doi: 10.1103/PhysRevLett.104.010503.
- [77] T. Wilk, A. Gaëtan, C. Evellin, J. Wolters, Y. Miroshnychenko, P. Grangier, and A. Browaeys. Entanglement of two individual neutral atoms using Rydberg blockade. *Physical Review Letters*, 104(1):010502, January 2010. ISSN 0031-9007, 1079-7114. doi: 10.1103/PhysRevLett.104.010502.
- [78] K. M. Maller, M. T. Lichtman, T. Xia, Y. Sun, M. J. Piotrowicz, A. W. Carr, L. Isenhower, and M. Saffman. Rydberg-blockade controlled-not gate and entanglement in a two-dimensional array of neutral-atom qubits. *Physical Review A*, 92(2):022336, August 2015. ISSN 1050-2947, 1094-1622. doi: 10.1103/PhysRevA.92.022336.
- [79] Harry Levine, Alexander Keesling, Giulia Semeghini, Ahmed Omran, Tout T. Wang, Sepehr Ebadi, Hannes Bernien, Markus Greiner, Vladan Vuletić, Hannes Pichler, and Mikhail D. Lukin. Parallel implementation of high-fidelity multi-qubit gates with neutral atoms. *Physical Review Letters*, 123(17):170503, October 2019. ISSN 0031-9007, 1079-7114. doi: 10.1103/PhysRevLett.123.170503.
- [80] Ivaylo S. Madjarov, Jacob P. Covey, Adam L. Shaw, Joonhee Choi, Anant Kale, Alexandre Cooper, Hannes Pichler, Vladimir Schkolnik, Jason R. Williams, and Manuel Endres. High-fidelity entanglement and detection of alkaline-earth Rydberg atoms. *Nature Physics*, 16(8):857–861, August 2020. ISSN 1745-2473, 1745-2481. doi: 10.1038/s41567-020-0903-z.
- [81] Pascal Scholl, Adam L. Shaw, Richard Bing-Shiun Tsai, Ran Finkelstein, Joonhee Choi, and Manuel Endres. Erasure conversion in a high-fidelity Rydberg quantum simulator. *Nature*, 622(7982):273–278, October 2023. ISSN 0028-0836, 1476-4687. doi: 10.1038/s41586-023-06516-4.
- [82] Simon J. Evered, Dolev Bluvstein, Marcin Kalinowski, Sepehr Ebadi, Tom Manovitz, Hengyun Zhou, Sophie H. Li, Alexandra A. Geim, Tout T. Wang, Nishad Maskara, Harry Levine, Giulia Semeghini, Markus Greiner, Vladan Vuletić, and Mikhail D. Lukin. High-fidelity parallel entangling gates on a neutral-atom quantum computer. *Nature*, 622(7982):268–272, October 2023. ISSN 0028-0836, 1476-4687. doi: 10.1038/s41586-023-06481-y.
- [83] J. A. Muniz, et al. High-Fidelity Universal Gates in the  $^{171}\text{Yb}$  Ground-State Nuclear-Spin Qubit. *PRX Quantum*, 6(2):020334, May 2025. doi: 10.1103/PRXQuantum.6.020334.
- [84] Michael Peper, Yiyi Li, Daniel Y. Knapp, Mila Bileska, Shuo Ma, Genyue Liu, Pai Peng, Bichen Zhang, Sebastian P. Horvath, Alex P. Burgers, and Jeff D. Thompson. Spectroscopy and Modeling of  $^{171}\text{Yb}$  Rydberg States for High-Fidelity Two-Qubit Gates. *Physical Review X*, 15(1):011009, January 2025. doi: 10.1103/PhysRevX.15.011009.
- [85] Richard Bing-Shiun Tsai, Xiangkai Sun, Adam L. Shaw, Ran Finkelstein, and Manuel Endres. Benchmarking and Fidelity Response Theory of High-Fidelity Rydberg Entangling Gates. *PRX Quantum*, 6(1):010331, February 2025. doi: 10.1103/PRXQuantum.6.010331.
- [86] A. G. Radnaev, et al. A universal neutral-atom quantum computer with individual optical addressing and non-destructive readout. January 2025. doi: 10.48550/arXiv.2408.08288.
- [87] C. A. Sackett, D. Kielpinski, B. E. King, C. Langer, V. Meyer, C. J. Myatt, M. Rowe, Q. A. Turchette, W. M. Itano, D. J. Wineland, and C. Monroe. Experimental entanglement of four particles. *Nature*, 404(6775):256–259, March 2000. ISSN 1476-4687. doi: 10.1038/35005011.
- [88] M. A. Rowe, D. Kielpinski, V. Meyer, C. A. Sackett, W. M. Itano, C. Monroe, and D. J. Wineland. Experimental violation of a Bell’s inequality with efficient detection. *Nature*, 409(6822):791–794, February 2001. ISSN 1476-4687. doi: 10.1038/35057215.

- [89] D. Leibfried, B. DeMarco, V. Meyer, D. Lucas, M. Barrett, J. Britton, W. M. Itano, B. Jelenković, C. Langer, T. Rosenband, and D. J. Wineland. Experimental demonstration of a robust, high-fidelity geometric two ion-qubit phase gate. *Nature*, 422(6930):412–415, March 2003. ISSN 1476-4687. doi: 10.1038/nature01492.
- [90] H. Häffner, F. Schmidt-Kaler, W. Hänsel, C. F. Roos, T. Körber, M. Chwalla, M. Riebe, J. Benhelm, U. D. Rapol, C. Becher, and R. Blatt. Robust entanglement. *Applied Physics B*, 81(2):151–153, July 2005. ISSN 1432-0649. doi: 10.1007/s00340-005-1917-z.
- [91] J. Benhelm, G. Kirchmair, C. F. Roos, and R. Blatt. Towards fault-tolerant quantum computing with trapped ions. *Nature Physics*, 4(6):463–466, June 2008. ISSN 1745-2473, 1745-2481. doi: 10.1038/nphys961.
- [92] C. J. Ballance, T. P. Harty, N. M. Linke, M. A. Sepiol, and D. M. Lucas. High-fidelity quantum logic gates using trapped-ion hyperfine qubits. *Physical Review Letters*, 117(6):060504, August 2016. ISSN 0031-9007, 1079-7114. doi: 10.1103/PhysRevLett.117.060504.
- [93] J. P. Gaebler, T. R. Tan, Y. Lin, Y. Wan, R. Bowler, A. C. Keith, S. Glancy, K. Coakley, E. Knill, D. Leibfried, and D. J. Wineland. High-Fidelity Universal Gate Set for  ${}^9\text{Be}^+$  Ion Qubits. *Physical Review Letters*, 117(6):060505, August 2016. ISSN 0031-9007, 1079-7114. doi: 10.1103/PhysRevLett.117.060505.
- [94] C. M. Löschauer, J. Mosca Toba, A. C. Hughes, S. A. King, M. A. Weber, R. Srinivas, R. Matt, R. Nourshargh, D. T. C. Allcock, C. J. Ballance, C. Matthiesen, M. Malinowski, and T. P. Harty. Scalable, high-fidelity all-electronic control of trapped-ion qubits. July 2024. doi: 10.48550/arXiv.2407.07694.
- [95] W. Huang, C. H. Yang, K. W. Chan, T. Tanttu, B. Hensen, R. C. C. Leon, M. A. Fogarty, J. C. C. Hwang, F. E. Hudson, K. M. Itoh, A. Morello, A. Laucht, and A. S. Dzurak. Fidelity benchmarks for two-qubit gates in silicon. *Nature*, 569(7757):532–536, May 2019. ISSN 1476-4687. doi: 10.1038/s41586-019-1197-0.
- [96] Akito Noiri, Kenta Takeda, Takashi Nakajima, Takashi Kobayashi, Amir Sammak, Giordano Scappucci, and Seigo Tarucha. Fast universal quantum control above the fault-tolerance threshold in silicon. *Nature*, 601(7893):338–342, January 2022. ISSN 0028-0836, 1476-4687. doi: 10.1038/s41586-021-04182-y.
- [97] Xiao Xue, Maximilian Russ, Nodar Samkharadze, Brennan Undseth, Amir Sammak, Giordano Scappucci, and Lieven M. K. Vandersypen. Quantum logic with spin qubits crossing the surface code threshold. *Nature*, 601(7893):343–347, January 2022. ISSN 1476-4687. doi: 10.1038/s41586-021-04273-w.
- [98] Takashi Yamamoto, Christoph Müller, Liam P. McGuinness, Tokuyuki Teraji, Boris Naydenov, Shinobu Onoda, Takeshi Ohshima, Jörg Wrachtrup, Fedor Jelezko, and Junichi Isoya. Strongly coupled diamond spin qubits by molecular nitrogen implantation. *Physical Review B*, 88(20):201201, November 2013. doi: 10.1103/PhysRevB.88.201201.
- [99] Thomas Monz, Philipp Schindler, Julio T. Barreiro, Michael Chwalla, Daniel Nigg, William A. Coish, Maximilian Harlander, Wolfgang Hänsel, Markus Henrich, and Rainer Blatt. 14-qubit entanglement: Creation and coherence. *Physical Review Letters*, 106(13):130506, March 2011. ISSN 0031-9007, 1079-7114. doi: 10.1103/PhysRevLett.106.130506.
- [100] Nicolai Friis, Oliver Marty, Christine Maier, Cornelius Hempel, Milan Holzapfel, Petar Jurcevic, Martin B. Plenio, Marcus Huber, Christian Roos, Rainer Blatt, and Ben Lanyon. Observation of Entangled States of a Fully Controlled 20-Qubit System. *Physical Review X*, 8(2):021012, April 2018. ISSN 2160-3308. doi: 10.1103/PhysRevX.8.021012.
- [101] Dominik Kiesenhofer, Helene Hainzer, Artem Zhdanov, Philip C. Holz, Matthias Bock, Tuomas Ollikainen, and Christian F. Roos. Controlling two-dimensional Coulomb crystals of more than 100 ions in a monolithic radio-frequency trap. *PRX Quantum*, 4(2):020317, April 2023. ISSN 2691-3399. doi: 10.1103/PRXQuantum.4.020317.
- [102] Daniel Barredo, Sylvain De Léséleuc, Vincent Lienhard, Thierry Lahaye, and Antoine Browaeys. An atom-by-atom assembler of defect-free arbitrary two-dimensional atomic arrays. *Science*, 354(6315):1021–1023, November 2016. ISSN 0036-8075, 1095-9203. doi: 10.1126/science.aah3778.
- [103] Hannes Bernien, Sylvain Schwartz, Alexander Keesling, Harry Levine, Ahmed Omran, Hannes Pichler, Soonwon Choi, Alexander S. Zibrov, Manuel Endres, Markus Greiner, Vladan Vuletić, and Mikhail D. Lukin. Probing many-body dynamics on a 51-atom quantum simulator. *Nature*, 551(7682):579–584, November 2017. ISSN 0028-0836, 1476-4687. doi: 10.1038/nature24622.

- [104] Daniel Ohl de Mello, Dominik Schäffner, Jan Werkmann, Tilman Preuschoff, Lars Kohfahl, Malte Schlosser, and Gerhard Birkl. Defect-free assembly of 2D clusters of more than 100 single-atom quantum systems. *Physical Review Letters*, 122(20):203601, May 2019. ISSN 0031-9007, 1079-7114. doi: 10.1103/PhysRevLett.122.203601.
- [105] Sepehr Ebadi, Tout T. Wang, Harry Levine, Alexander Keesling, Giulia Semeghini, Ahmed Omran, Dolev Bluvstein, Rhine Samajdar, Hannes Pichler, Wen Wei Ho, Soonwon Choi, Subir Sachdev, Markus Greiner, Vladan Vuletić, and Mikhail D. Lukin. Quantum phases of matter on a 256-atom programmable quantum simulator. *Nature*, 595(7866):227–232, July 2021. ISSN 0028-0836, 1476-4687. doi: 10.1038/s41586-021-03582-4.
- [106] Kai-Niklas Schymik, Bruno Ximenez, Etienne Bloch, Davide Dreon, Adrien Signoles, Florence Nogrette, Daniel Barredo, Antoine Browaeys, and Thierry Lahaye. In-situ equalization of single-atom loading in large-scale optical tweezers arrays. *Physical Review A*, 106(2):022611, August 2022. ISSN 2469-9926, 2469-9934. doi: 10.1103/PhysRevA.106.022611.
- [107] Rui Lin, Han-Sen Zhong, You Li, Zhang-Rui Zhao, Le-Tian Zheng, Tai-Ran Hu, Hong-Ming Wu, Zhan Wu, Wei-Jie Ma, Yan Gao, Yi-Kang Zhu, Zhao-Feng Su, Wan-Li Ouyang, Yu-Chen Zhang, Jun Rui, Ming-Cheng Chen, Chao-Yang Lu, and Jian-Wei Pan. AI-Enabled Rapid Assembly of Thousands of Defect-Free Neutral Atom Arrays with Constant-time-overhead. December 2024. doi: 10.48550/arXiv.2412.14647.
- [108] Grégoire Pichard, Desiree Lim, Étienne Bloch, Julien Vaneechloo, Lilian Bourachot, Gert-Jan Both, Guillaume Mériaux, Sylvain Dutartre, Richard Hostein, Julien Paris, Bruno Ximenez, Adrien Signoles, Antoine Browaeys, Thierry Lahaye, and Davide Dreon. Rearrangement of individual atoms in a 2000-site optical-tweezer array at cryogenic temperatures. *Physical Review Applied*, 22(2):024073, August 2024. doi: 10.1103/PhysRevApplied.2.2.024073.
- [109] Jerry M. Chow, Jay M. Gambetta, Easwar Magesan, David W. Abraham, Andrew W. Cross, B. R. Johnson, Nicholas A. Masluk, Colm A. Ryan, John A. Smolin, Srikanth J. Srinivasan, and M. Steffen. Implementing a strand of a scalable fault-tolerant quantum computing fabric. *Nature Communications*, 5(1), June 2014. doi: 10.1038/ncomms5015.
- [110] R. Barends, J. Kelly, A. Megrant, A. Veitia, D. Sank, E. Jeffrey, T. C. White, J. Mutus, A. G. Fowler, B. Campbell, Y. Chen, Z. Chen, B. Chiaro, A. Dunsworth, C. Neill, P. O’Malley, P. Roushan, A. Vainsencher, J. Wenner, A. N. Korotkov, A. N. Cleland, and John M. Martinis. Superconducting quantum circuits at the surface code threshold for fault tolerance. *Nature*, 508(7497):500–503, April 2014. doi: 10.1038/nature13171.
- [111] Arute, et al. Quantum supremacy using a programmable superconducting processor. *Nature*, 574(7779):505–510, October 2019. ISSN 1476-4687. doi: 10.1038/s41586-019-1666-5.
- [112] Youngseok Kim, Andrew Eddins, Sajant Anand, Ken Xuan Wei, Ewout van den Berg, Sami Rosenblatt, Hasan Nayfeh, Yantao Wu, Michael Zaletel, Kristan Temme, and Abhinav Kandala. Evidence for the utility of quantum computing before fault tolerance. *Nature*, 618(7965):500–505, June 2023. ISSN 1476-4687. doi: 10.1038/s41586-023-06096-3.
- [113] T. F. Watson, S. G. J. Philips, E. Kawakami, D. R. Ward, P. Scarlino, M. Veldhorst, D. E. Savage, M. G. Lagally, Mark Friesen, S. N. Coppersmith, M. A. Eriksson, and L. M. K. Vandersypen. A programmable two-qubit quantum processor in silicon. *Nature*, 555(7698):633–637, March 2018. ISSN 0028-0836, 1476-4687. doi: 10.1038/nature25766.
- [114] Nico W. Hendrickx, William I. L. Lawrie, Maximilian Russ, Floor van Riggelen, Sander L. de Snoo, Raymond N. Schouten, Amir Sammak, Giordano Scappucci, and Menno Veldhorst. A four-qubit germanium quantum processor. *Nature*, 591(7851):580–585, March 2021. ISSN 1476-4687. doi: 10.1038/s41586-021-03332-6.
- [115] Stephan G. J. Philips, Mateusz T. Mądzik, Sergey V. Amitonov, Sander L. de Snoo, Maximilian Russ, Nima Kalhor, Christian Volk, William I. L. Lawrie, Delphine Brousse, Larysa Tryputen, Brian Paquette Wuetz, Amir Sammak, Menno Veldhorst, Giordano Scappucci, and Lieven M. K. Vandersypen. Universal control of a six-qubit quantum processor in silicon. *Nature*, 609(7929):919–924, September 2022. ISSN 0028-0836, 1476-4687. doi: 10.1038/s41586-022-05117-x.
- [116] C. E. Bradley. A Ten-Qubit Solid-State Spin Register with Quantum Memory up to One Minute. *Physical Review X*, 9(3), 2019. doi: 10.1103/PhysRevX.9.031045.
- [117] Daniel Gottesman. Quantum fault tolerance in small experiments. October 2016. doi: 10.48550/arXiv.1610.03507.

- [118] Raymond Laflamme, Cesar Miquel, Juan Pablo Paz, and Wojciech Hubert Zurek. Perfect Quantum Error Correcting Code. *Physical Review Letters*, 77(1):198–201, July 1996. doi: 10.1103/PhysRevLett.77.198.
- [119] Charles H. Bennett, David P. DiVincenzo, John A. Smolin, and William K. Wootters. Mixed State Entanglement and Quantum Error Correction. *Physical Review A*, 54(5):3824–3851, November 1996. ISSN 1050-2947, 1094-1622. doi: 10.1103/PhysRevA.54.3824.
- [120] A. R. Calderbank and Peter W. Shor. Good Quantum Error-Correcting Codes Exist. *Physical Review A*, 54(2):1098–1105, August 1996. ISSN 1050-2947, 1094-1622. doi: 10.1103/PhysRevA.54.1098.
- [121] E. Knill, R. Laflamme, and G. J. Milburn. A scheme for efficient quantum computation with linear optics. *Nature*, 409(6816):46–52, January 2001. ISSN 1476-4687. doi: 10.1038/35051009.
- [122] Victor V. Albert and Philippe Faist. Quantum repetition code. [https://errorcorrectionzoo.org/c/quantum\\_repetition](https://errorcorrectionzoo.org/c/quantum_repetition), 2022.
- [123] J. Chiaverini, D. Leibfried, T. Schaetz, M. D. Barrett, R. B. Blakestad, J. Britton, W. M. Itano, J. D. Jost, E. Knill, C. Langer, R. Ozeri, and D. J. Wineland. Realization of quantum error correction. *Nature*, 432(7017):602–605, December 2004. ISSN 1476-4687. doi: 10.1038/nature03074.
- [124] Osama Moussa, Jonathan Baugh, Colm A. Ryan, and Raymond Laflamme. Demonstration of sufficient control for two rounds of quantum error correction in a solid state ensemble quantum information processor. *Physical Review Letters*, 107(16):160501, October 2011. ISSN 0031-9007, 1079-7114. doi: 10.1103/PhysRevLett.107.160501.
- [125] M. D. Reed, L. DiCarlo, S. E. Nigg, L. Sun, L. Frunzio, S. M. Girvin, and R. J. Schoelkopf. Realization of three-qubit quantum error correction with superconducting circuits. *Nature*, 482(7385):382–385, February 2012. ISSN 1476-4687. doi: 10.1038/nature10786.
- [126] Philipp Schindler, Julio T. Barreiro, Thomas Monz, Volckmar Nebendahl, Daniel Nigg, Michael Chwalla, Markus Hennrich, and Rainer Blatt. Experimental Repetitive Quantum Error Correction. *Science*, 332(6033):1059–1061, May 2011. doi: 10.1126/science.1203329.
- [127] Jingfu Zhang, Dorian Gangloff, Osama Moussa, and Raymond Laflamme. Experimental quantum error correction with high fidelity. *Physical Review A*, 84(3):034303, September 2011. ISSN 1050-2947, 1094-1622. doi: 10.1103/PhysRevA.84.034303.
- [128] G. Waldherr, Y. Wang, S. Zaiser, M. Jamali, T. Schulte-Herbrueggen, H. Abe, T. Ohshima, J. Isoya, P. Neumann, and J. Wrachtrup. Quantum error correction in a solid-state hybrid spin register. *Nature*, 506(7487):204–207, February 2014. ISSN 0028-0836, 1476-4687. doi: 10.1038/nature12919.
- [129] J. Kelly, R. Barends, A. G. Fowler, A. Megrant, E. Jeffrey, T. C. White, D. Sank, J. Y. Mutus, B. Campbell, Yu Chen, Z. Chen, B. Chiaro, A. Dunsworth, I.-C. Hoi, C. Neill, P. J. J. O’Malley, C. Quintana, P. Roushan, A. Vainsencher, J. Wenner, A. N. Cleland, and John M. Martinis. State preservation by repetitive error detection in a superconducting quantum circuit. *Nature*, 519(7541):66–69, March 2015. doi: 10.1038/nature14270.
- [130] D. Ristè, S. Poletto, M.-Z. Huang, A. Bruno, V. Vesterinen, O.-P. Saira, and L. DiCarlo. Detecting bit-flip errors in a logical qubit using stabilizer measurements. *Nature Communications*, 6(1), April 2015. doi: 10.1038/ncomms7983.
- [131] Julia Cramer, Norbert Kalb, M. Adriaan Rol, Bas Hensen, Machiel S. Blok, Matthew Markham, Daniel J. Twitchen, Ronald Hanson, and Tim H. Taminiau. Repeated quantum error correction on a continuously encoded qubit by real-time feedback. *Nature Communications*, 7(1):11526, May 2016. ISSN 2041-1723. doi: 10.1038/ncomms11526.
- [132] James R. Wootton and Daniel Loss. A repetition code of 15 qubits. *Physical Review A*, 97(5):052313, May 2018. ISSN 2469-9926, 2469-9934. doi: 10.1103/PhysRevA.97.052313.
- [133] James R Wootton. Benchmarking near-term devices with quantum error correction. *Quantum Science and Technology*, 5(4):044004, October 2020. ISSN 2058-9565. doi: 10.1088/2058-9565/aba038.
- [134] Google Quantum AI Exponential suppression of bit or phase errors with cyclic error correction. *Nature*, 595(7867):383–387, July 2021. ISSN 0028-0836, 1476-4687. doi: 10.1038/s41586-021-03588-y.

- [135] Google Quantum AI Suppressing quantum errors by scaling a surface code logical qubit. *Nature*, 614(7949): 676–681, February 2023. doi: 10.1038/s41586-022-05434-1.
- [136] Google Quantum AI and Collaborators Quantum error correction below the surface code threshold. *Nature*, 638(8052):920–926, February 2025. ISSN 0028-0836, 1476-4687. doi: 10.1038/s41586-024-08449-y.
- [137] Puterman, et al. Hardware-efficient quantum error correction via concatenated bosonic qubits. *Nature*, 638 (8052):927–934, February 2025. ISSN 1476-4687. doi: 10.1038/s41586-025-08642-7.
- [138] E. Knill, R. Laflamme, R. Martinez, and C. Negrevergne. Implementation of the Five Qubit Error Correction Benchmark. *Physical Review Letters*, 86(25):5811–5814, June 2001. ISSN 0031-9007, 1079-7114. doi: 10.1103/PhysRevLett.86.5811.
- [139] Jingfu Zhang, Raymond Laflamme, and Dieter Suter. Experimental implementation of encoded logical qubit operations in a perfect quantum error correcting code. *Physical Review Letters*, 109(10):100503, September 2012. ISSN 0031-9007, 1079-7114. doi: 10.1103/PhysRevLett.109.100503.
- [140] Ming Gong, Xiao Yuan, Shiyu Wang, Yulin Wu, Youwei Zhao, Chen Zha, Shaowei Li, Zhen Zhang, Qi Zhao, Yunchao Liu, Futian Liang, Jin Lin, Yu Xu, Hui Deng, Hao Rong, He Lu, Simon C. Benjamin, Cheng-Zhi Peng, Xiongfeng Ma, Yu-Ao Chen, Xiaobo Zhu, and Jian-Wei Pan. Experimental exploration of five-qubit quantum error correcting code with superconducting qubits. *National Science Review*, 9(1):nwab011, January 2022. ISSN 2095-5138, 2053-714X. doi: 10.1093/nsr/nwab011.
- [141] N. M. Linke, M. Gutierrez, K. A. Landsman, C. Figgatt, S. Debnath, K. R. Brown, and C. Monroe. Fault-tolerant quantum error detection. *Science Advances*, 3(10):e1701074, October 2017. ISSN 2375-2548. doi: 10.1126/sciadv.1701074.
- [142] Maika Takita, Andrew W. Cross, A. D. Córcoles, Jerry M. Chow, and Jay M. Gambetta. Experimental Demonstration of Fault-Tolerant State Preparation with Superconducting Qubits. *Physical Review Letters*, 119(18):180501, October 2017. doi: 10.1103/PhysRevLett.119.180501.
- [143] Joschka Roffe, David Headley, Nicholas Chancellor, Dominic Horsman, and Viv Kendon. Protecting quantum memories using coherent parity check codes. *Quantum Science and Technology*, 3(3):035010, July 2018. ISSN 2058-9565. doi: 10.1088/2058-9565/aac64e.
- [144] D. Willsch, M. Willsch, F. Jin, H. De Raedt, and K. Michielsen. Testing quantum fault tolerance on small systems. *Physical Review A*, 98(5):052348, November 2018. ISSN 2469-9926, 2469-9934. doi: 10.1103/PhysRevA.98.052348.
- [145] Christophe Vuillot. Is error detection helpful on IBM 5Q chips ? *Quantum Information and Computation*, 18 (11&12), 2018. ISSN 15337146, 15337146. doi: 10.26421/QIC18.11-12.
- [146] Robin Harper and Steven T. Flammia. Fault-Tolerant Logical Gates in the IBM Quantum Experience. *Physical Review Letters*, 122(8):080504, February 2019. ISSN 0031-9007, 1079-7114. doi: 10.1103/PhysRevLett.122.080504.
- [147] Abhoy Kole and Indranil Sengupta. Resource Optimal Realization of Fault-Tolerant Quantum Circuit. In *2020 IEEE International Test Conference India*, pages 1–10, July 2020. doi: 10.1109/ITCIndia49857.2020.9171796.
- [148] Kai Sun, Ze-Yan Hao, Yan Wang, Jia-Kun Li, Xiao-Ye Xu, Jin-Shi Xu, Yong-Jian Han, Chuan-Feng Li, and Guang-Can Guo. Optical demonstration of quantum fault-tolerant threshold. *Light: Science & Applications*, 11(1):203, July 2022. ISSN 2047-7538. doi: 10.1038/s41377-022-00891-9.
- [149] Miroslav Urbanek, Benjamin Nachman, and Wibe A. de Jong. Error detection on quantum computers improves accuracy of chemical calculations. *Physical Review A*, 102(2):022427, August 2020. ISSN 2469-9926, 2469-9934. doi: 10.1103/PhysRevA.102.022427.
- [150] Rosie Cane, Daryus Chandra, Soon Xin Ng, and Lajos Hanzo. Experimental Characterization of Fault-Tolerant Circuits in Small-Scale Quantum Processors. *IEEE Access*, 9:162996–163011, 2021. ISSN 2169-3536. doi: 10.1109/ACCESS.2021.3133483.
- [151] Shaobo Zhang, Charles D. Hill, and Muhammad Usman. Comparative analysis of error mitigation techniques for variational quantum eigensolver implementations on IBM quantum system. June 2022. doi: 10.48550/arXiv.2206.07907.

- [152] Matt J. Bedalov, Matt Blakely, Peter D. Buttler, Caitlin Carnahan, Frederic T. Chong, Woo Chang Chung, Dan C. Cole, Palash Goiporia, Pranav Gokhale, Bettina Heim, Garrett T. Hickman, Eric B. Jones, Ryan A. Jones, Pradnya Khalate, Jin-Sung Kim, Kevin W. Kuper, Martin T. Lichtman, Stephanie Lee, David Mason, Nathan A. Neff-Mallon, Thomas W. Noel, Victory Omole, Alexander G. Radnaev, Rich Rines, Mark Saffman, Efrat Shabtai, Mariesa H. Teo, Bharath Thotakura, Teague Tomesh, and Angela K. Tucker. Fault-Tolerant Operation and Materials Science with Neutral Atom Logical Qubits. December 2024. doi: 10.48550/arXiv.2412.07670.
- [153] Wim van Dam, Hongbin Liu, Guang Hao Low, Adam Paetznick, Andres Paz, Marcus Silva, Aarthi Sundaram, Krysta Svore, and Matthias Troyer. End-to-End Quantum Simulation of a Chemical System. September 2024. doi: 10.48550/arXiv.2409.05835.
- [154] Riddhi S. Gupta, Neereja Sundaresan, Thomas Alexander, Christopher J. Wood, Seth T. Merkel, Michael B. Healy, Marius Hillenbrand, Tomas Jochym-O'Connor, James R. Wootton, Theodore J. Yoder, Andrew W. Cross, Maika Takita, and Benjamin J. Brown. Encoding a magic state with beyond break-even fidelity. *Nature*, 625(7994):259–263, January 2024. ISSN 0028-0836, 1476-4687. doi: 10.1038/s41586-023-06846-3.
- [155] Reichardt, et al. Logical computation demonstrated with a neutral atom quantum processor. November 2024. doi: 10.48550/arXiv.2411.11822.
- [156] Victor V. Albert and Philippe Faist. Rotated surface code. [https://errorcorrectionzoo.org/c/rotated\\_surface](https://errorcorrectionzoo.org/c/rotated_surface), 2024.
- [157] B. A. Bell, D. A. Herrera-Martí, M. S. Tame, D. Markham, W. J. Wadsworth, and J. G. Rarity. Experimental demonstration of a graph state quantum error-correction code. *Nature Communications*, 5(1):3658, April 2014. ISSN 2041-1723. doi: 10.1038/ncomms4658.
- [158] Christian Kraglund Andersen, Ants Remm, Stefania Lazar, Sebastian Krinner, Nathan Lacroix, Graham J. Norris, Mihai Gabureac, Christopher Eichler, and Andreas Wallraff. Repeated quantum error detection in a surface code. *Nature Physics*, 16(8):875–880, June 2020. doi: 10.1038/s41567-020-0920-y.
- [159] Sebastian Krinner, Nathan Lacroix, Ants Remm, Agustin Di Paolo, Elie Genois, Catherine Leroux, Christoph Hellings, Stefania Lazar, Francois Swiadek, Johannes Herrmann, Graham J. Norris, Christian Kraglund Andersen, Markus Müller, Alexandre Blais, Christopher Eichler, and Andreas Wallraff. Realizing repeated quantum error correction in a distance-three surface code. *Nature*, 605(7911):669–674, May 2022. doi: 10.1038/s41586-022-04566-8.
- [160] Dolev Bluvstein, Simon J. Evered, Alexandra A. Geim, Sophie H. Li, Hengyun Zhou, Tom Manovitz, Sepehr Ebadi, Madelyn Cain, Marcin Kalinowski, Dominik Hangleiter, J. Pablo Bonilla Ataides, Nishad Maskara, Iris Cong, Xun Gao, Pedro Sales Rodriguez, Thomas Karolyshyn, Giulia Semeghini, Michael J. Gullans, Markus Greiner, Vladan Vuletić, and Mikhail D. Lukin. Logical quantum processor based on reconfigurable atom arrays. *Nature*, 626(7997):58–65, February 2024. ISSN 0028-0836, 1476-4687. doi: 10.1038/s41586-023-06927-3.
- [161] Eickbusch, et al. Demonstrating dynamic surface codes. December 2024. doi: 10.48550/arXiv.2412.14360.
- [162] Daniel Nigg, Markus Mueller, Esteban A. Martinez, Philipp Schindler, Markus Hennrich, Thomas Monz, Miguel A. Martin-Delgado, and Rainer Blatt. Experimental Quantum Computations on a Topologically Encoded Qubit. *Science*, 345(6194):302–305, July 2014. ISSN 0036-8075, 1095-9203. doi: 10.1126/science.1253742.
- [163] Lacroix, et al. Scaling and logic in the color code on a superconducting quantum processor. December 2024. doi: 10.48550/arXiv.2412.14256.
- [164] Rodriguez, et al. Experimental Demonstration of Logical Magic State Distillation. December 2024. doi: 10.48550/arXiv.2412.15165.
- [165] D. Bacon. Decoherence, Control, and Symmetry in Quantum Computers. May 2003. doi: 10.48550/arXiv.quant-ph/0305025.
- [166] Dave Bacon. Operator Quantum Error Correcting Subsystems for Self-Correcting Quantum Memories. *Physical Review A*, 73(1):012340, January 2006. ISSN 1050-2947, 1094-1622. doi: 10.1103/PhysRevA.73.012340.
- [167] Laird Egan, Dripto M. Debroy, Crystal Noel, Andrew Risinger, Daiwei Zhu, Debopriyo Biswas, Michael Newman, Muyuan Li, Kenneth R. Brown, Marko Cetina, and Christopher Monroe. Fault-tolerant control of an error-corrected qubit. *Nature*, 598(7880):281–286, October 2021. ISSN 1476-4687. doi: 10.1038/s41586-021-03928-y.

- [168] Yi-Han Luo, Ming-Cheng Chen, Manuel Erhard, Han-Sen Zhong, Dian Wu, Hao-Yang Tang, Qi Zhao, Xi-Lin Wang, Keisuke Fujii, Li Li, Nai-Le Liu, Kae Nemoto, William J. Munro, Chao-Yang Lu, Anton Zeilinger, and Jian-Wei Pan. Quantum teleportation of physical qubits into logical code-spaces. *Proceedings of the National Academy of Sciences*, 118(36):e2026250118, September 2021. ISSN 0027-8424, 1091-6490. doi: 10.1073/pnas.2026250118.
- [169] A. D. Córcoles, Easwar Magesan, Srikanth J. Srinivasan, Andrew W. Cross, M. Steffen, Jay M. Gambetta, and Jerry M. Chow. Demonstration of a quantum error detection code using a square lattice of four superconducting qubits. *Nature Communications*, 6(1):6979, April 2015. ISSN 2041-1723. doi: 10.1038/ncomms7979.
- [170] Christian Kraglund Andersen, Ants Remm, Stefania Lazar, Sebastian Krinner, Johannes Heinsoo, Jean-Claude Besse, Mihai Gabureac, Andreas Wallraff, and Christopher Eichler. Entanglement stabilization using ancilla-based parity detection and real-time feedback in superconducting circuits. *npj Quantum Information*, 5(1), August 2019. doi: 10.1038/s41534-019-0185-4.
- [171] C. C. Bultink, T. E. O'Brien, R. Vollmer, N. Muthusubramanian, M. W. Beekman, M. A. Rol, X. Fu, B. Tarasinski, V. Ostroukh, B. Varbanov, A. Bruno, and L. DiCarlo. Protecting quantum entanglement from leakage and qubit errors via repetitive parity measurements. *Science Advances*, 6(12), March 2020. doi: 10.1126/sciadv.aay3050.
- [172] Sergei Bravyi and Alexei Kitaev. Universal Quantum Computation with ideal Clifford gates and noisy ancillas. *Physical Review A*, 71(2):022316, February 2005. ISSN 1050-2947, 1094-1622. doi: 10.1103/PhysRevA.71.022316.
- [173] Craig Gidney, Noah Shutty, and Cody Jones. Magic state cultivation: Growing T states as cheap as CNOT gates. September 2024. doi: 10.48550/arXiv.2409.17595.
- [174] Moses, et al. A Race Track Trapped-Ion Quantum Processor. *Physical Review X*, 13(4):041052, December 2023. ISSN 2160-3308. doi: 10.1103/PhysRevX.13.041052.
- [175] Zehang Bao, Shibo Xu, Zixuan Song, Ke Wang, Liang Xiang, Zitian Zhu, Jiachen Chen, Feitong Jin, Xuhao Zhu, Yu Gao, Yaozu Wu, Chuanyu Zhang, Ning Wang, Yiren Zou, Ziqi Tan, Aosai Zhang, Zhengyi Cui, Fanhao Shen, Jiarun Zhong, Tingting Li, Jinfeng Deng, Xu Zhang, Hang Dong, Pengfei Zhang, Yang-Ren Liu, Liangtian Zhao, Jie Hao, Hekang Li, Zhen Wang, Chao Song, Qiujiang Guo, Biao Huang, and H. Wang. Creating and controlling global Greenberger-Horne-Zeilinger entanglement on quantum processors. *Nature Communications*, 15(1):8823, October 2024. ISSN 2041-1723. doi: 10.1038/s41467-024-53140-5.
- [176] Ben W. Reichardt, David Aasen, Rui Chao, Alex Chernoguzov, Wim van Dam, John P. Gaebler, Dan Gresh, Dominic Lucchetti, Michael Mills, Steven A. Moses, Brian Neyenhuis, Adam Paetznick, Andres Paz, Peter E. Siegfried, Marcus P. da Silva, Krysta M. Svore, Zhenghan Wang, and Matt Zanner. Demonstration of quantum computation and error correction with a tesseract code. December 2024. doi: 10.48550/arXiv.2409.04628.
- [177] Yifan Hong, Elijah Durso-Sabina, David Hayes, and Andrew Lucas. Entangling four logical qubits beyond break-even in a nonlocal code. *Physical Review Letters*, 133(18):180601, October 2024. ISSN 0031-9007, 1079-7114. doi: 10.1103/PhysRevLett.133.180601.
- [178] John Preskill. Beyond NISQ: The Meg aquop Machine. February 2025. doi: 10.48550/arXiv.2502.17368.
- [179] Pauli Virtanen, Ralf Gommers, Travis E. Oliphant, Matt Haberland, Tyler Reddy, David Cournapeau, Evgeni Burovski, Pearu Peterson, Warren Weckesser, Jonathan Bright, Stéfan J. van der Walt, Matthew Brett, Joshua Wilson, K. Jarrod Millman, Nikolay Mayorov, Andrew R. J. Nelson, Eric Jones, Robert Kern, Eric Larson, C. J. Carey, İlhan Polat, Yu Feng, Eric W. Moore, Jake VanderPlas, Denis Laxalde, Josef Perktold, Robert Cimrman, Ian Henriksen, E. A. Quintero, Charles R. Harris, Anne M. Archibald, Antônio H. Ribeiro, Fabian Pedregosa, and Paul van Mulbregt. SciPy 1.0: Fundamental algorithms for scientific computing in Python. *Nature Methods*, 17(3):261–272, March 2020. ISSN 1548-7105. doi: 10.1038/s41592-019-0686-2.

## 7 Appendices

### 7.1 Reaching the Utility Scale

To contextualize the physical qubit benchmarks within the broader goal of useful quantum computation [178], we project potential timelines towards a ‘utility scale’ regime, employing a working definition of achieving both

a Physical Qubit Count (PQC) of 10,000 and an Entanglement Error (EE) below 0.1% to be a factor 10 below the threshold of the surface code. These metrics are chosen somehow arbitrarily as being hard to reach but not impossible in near future and should be thought of as one possible scenario rather than the definition of utility. While individual gate errors (such as the two-qubit gate error) are commonly used to evaluate the distance to the accuracy threshold in QEC simulations, we use the entangled state error when it is the only available metric as it benchmarks the system’s capability to produce the high-fidelity entangled states essential for QEC, providing a functionally relevant and cross-platform comparable proxy for approaching fault-tolerance requirements. Besides, while one might specifically track the number of physical qubits directly employed within QEC code experiments (the focus of Section 3), examining the maximum reported physical qubit count remains a vital benchmark, as it reflects the underlying platform’s overall progress in fabrication, control, and potential scale, providing the resource pool from which future, larger QEC implementations must draw. By extrapolating the observed exponential improvement rates (halving times for EE, doubling times for PQC) summarized in Table 2, we can estimate when each platform might reach these specific thresholds.

**Table 2: Projected Utility-Scale (US) for Entanglement Error (EE) and Physical Qubit Count (PQC).** Best achieved (with corresponding year), doubling factor and estimated year of reaching the utility scale by platforms.

Platform	Best EE	Best EE Year	EE ÷2 factor	US EE	Best PQC	Best PQC Year	PQC ×2 factor	US PQC
Ion traps	0.0003	2024	2.4	<b>2024</b>	100	2023	5.0	<b>2056</b>
Neutral atoms	0.0020	2023	2.3	<b>2025</b>	6,100	2024	1.4	<b>2024</b>
Superconducting circuits	0.0030	2020	2.6	<b>2024</b>	127	2023	2.6	<b>2039</b>
Semiconductor spins	0.0035	2022	1.2	<b>2024</b>	6	2022	2.6	<b>2050</b>

This analysis projects that neutral atom platforms could satisfy both criteria as early as 2025, substantially sooner than trapped ions (projected for 2038) and superconducting circuits (2039). Within the assumptions of this model, the rapid PQC scaling factor currently observed for neutral atoms is the primary driver for this accelerated timeline.

However, several critical caveats apply to these projections. Firstly, let us emphasize again that the definition of ‘utility scale’ based solely on PQC and EE is a simplification: true utility will depend on a complex interplay of metrics including logical qubit fidelity, connectivity, gate speeds, and the ability to execute fault-tolerant protocols (as discussed in Section 3), not just raw physical qubit counts and error rates. The 10k and 0.1% target serves as one specific, potentially arbitrary, milestone. Secondly, the projection relies heavily on the assumption that current exponential scaling trends will continue for years or decades. Such extrapolations are inherently speculative, as technological progress may encounter unforeseen plateaus due to fundamental physics or engineering hurdles (as it seems to be already the case for the EE), or conversely, accelerate due to breakthroughs not captured by historical data. Factors like increasing crosstalk at scale, limitations in control systems, or shifts in research focus could significantly alter these trajectories. Therefore, while illustrative, these projections should be interpreted cautiously as reflecting potential timelines if current rates of progress persist and if the chosen PQC/EE targets adequately capture the requirements for utility.

## 7.2 Additional Visualisations

### 7.2.1 Yearly Experiment Counts by Platform

Complementing the cumulative view in Figure 4, Figure 6 displays the number of documented QEC-related experiments on a year-by-year basis, categorized by the experimental platform used. This non-cumulative representation highlights the annual research output and reveals trends in platform activity over time, such as the peak and subsequent decline of NMR contributions, the sustained output from trapped ions, and the recent acceleration of research using superconducting circuits and neutral atoms.

### 7.2.2 Cumulative Growth of QEC Implementations by Code Family

Figure 7 illustrates the cumulative number of reported experimental implementations specifically categorized by the family of QEC code employed, tracked over time. This view highlights which code families have received sustained

Yearly Experiment Counts by Platform

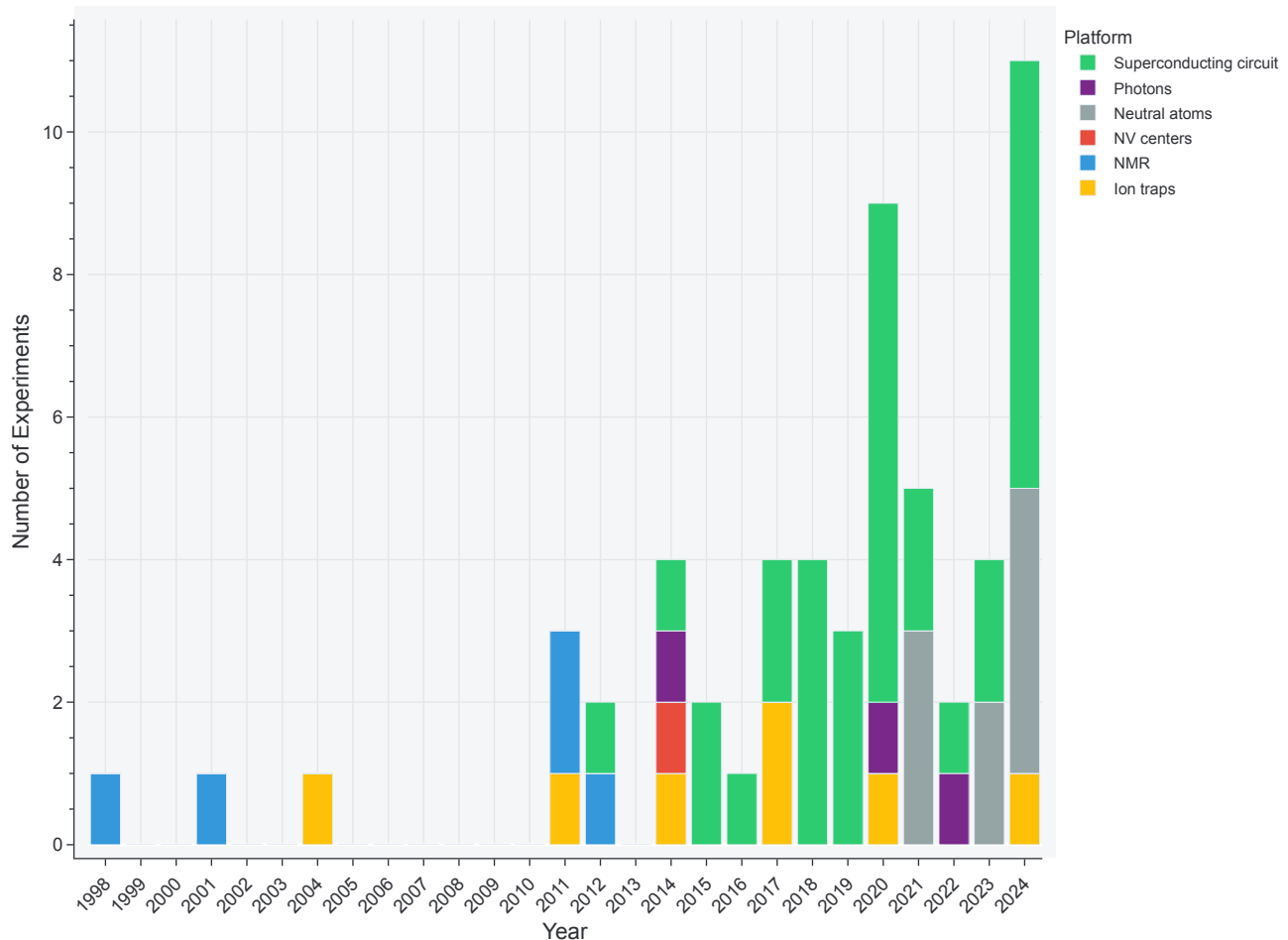


Figure 6: **Yearly experiment counts by platform.** Number of published QEC-related experiments per year, categorized by platform.

attention. Early activity is visible for central concepts demonstrated using Bell states and the  $[[5, 1, 3]]$  code. The plot shows significant recent growth in implementations of surface codes and repetition codes (often used as building blocks or testbeds for surface codes), along with substantial effort dedicated to four-qubit codes.

### 7.2.3 Timeline of Implementations

Figure 8 provides a detailed chronological perspective, mapping specific QEC code implementations (y-axis) to their publication year (x-axis) and indicating the platform used via color and shape. This visualization clearly shows the pioneering role of NMR in early demonstrations, the consistent contributions from trapped ion systems over many years, and the significant surge of activity in superconducting circuits and neutral atoms, particularly in the last decade. It also illustrates the progression towards implementing more complex codes, such as surface and color codes, primarily on these latter platforms.

### 7.2.4 Distribution of Implementations Across Platforms and Codes

The distribution of QEC experimental efforts across different hardware platforms and code types is summarized in the sunburst chart presented in Figure 9. The inner rings represent the physical platforms, while the outer rings show the specific QEC codes implemented, with segment sizes proportional to the number of documented experiments (indicated by counts). This reveals that superconducting circuits have hosted the largest volume and diversity

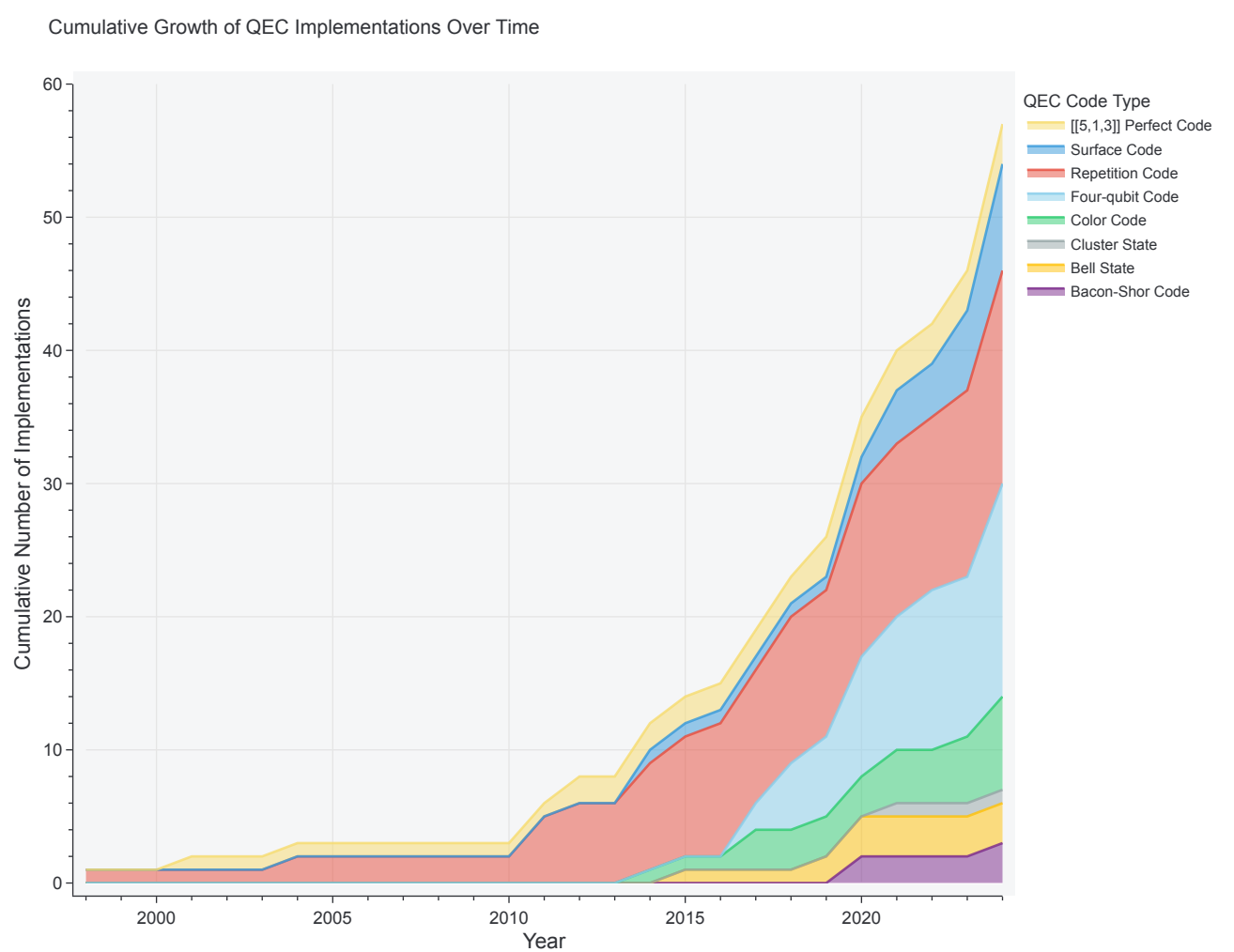


Figure 7: **Cumulative Growth of QEC Implementations.** Total number of reported experimental implementations for different QEC code families over time.

of QEC experiments to date, followed by trapped ions and, more recently, neutral atoms. It also highlights that certain codes, notably repetition codes and four-qubit codes, have been realized across multiple platforms, offering opportunities for cross-platform comparison. In contrast, implementations of larger-scale topological codes (e.g., surface, color codes with higher distances) are currently concentrated on platforms demonstrating higher available qubit counts.

### 7.3 Goodness of Fit for Exponential Trends

This appendix details the methodology used to assess how well the exponential trend lines, presented in Section 2.2 for physical qubit benchmarks (Figure 1, Figure 2, Figure 3), fit the collected historical experimental data.

#### 7.3.1 Methodology

To model the observed trends in coherence times ( $T_1, T_2$ ), entanglement error, and physical qubit count over time (year,  $x$ ), we assumed an exponential relationship of the form:  $y = A \cdot B^x$  where  $y$  represents the metric being analyzed. This exponential model can be linearized by applying a (base-10) logarithm:  $\log_{10}(y) = \log_{10}(A) + x \cdot \log_{10}(B)$ . This transformation yields a linear equation  $Y = c + m \cdot x$ , where  $Y = \log_{10}(y)$ , the intercept  $c = \log_{10}(A)$ , and the slope  $m = \log_{10}(B)$ .

Standard linear regression was performed on this transformed data (year vs.  $\log_{10}(\text{metric})$ ) using the

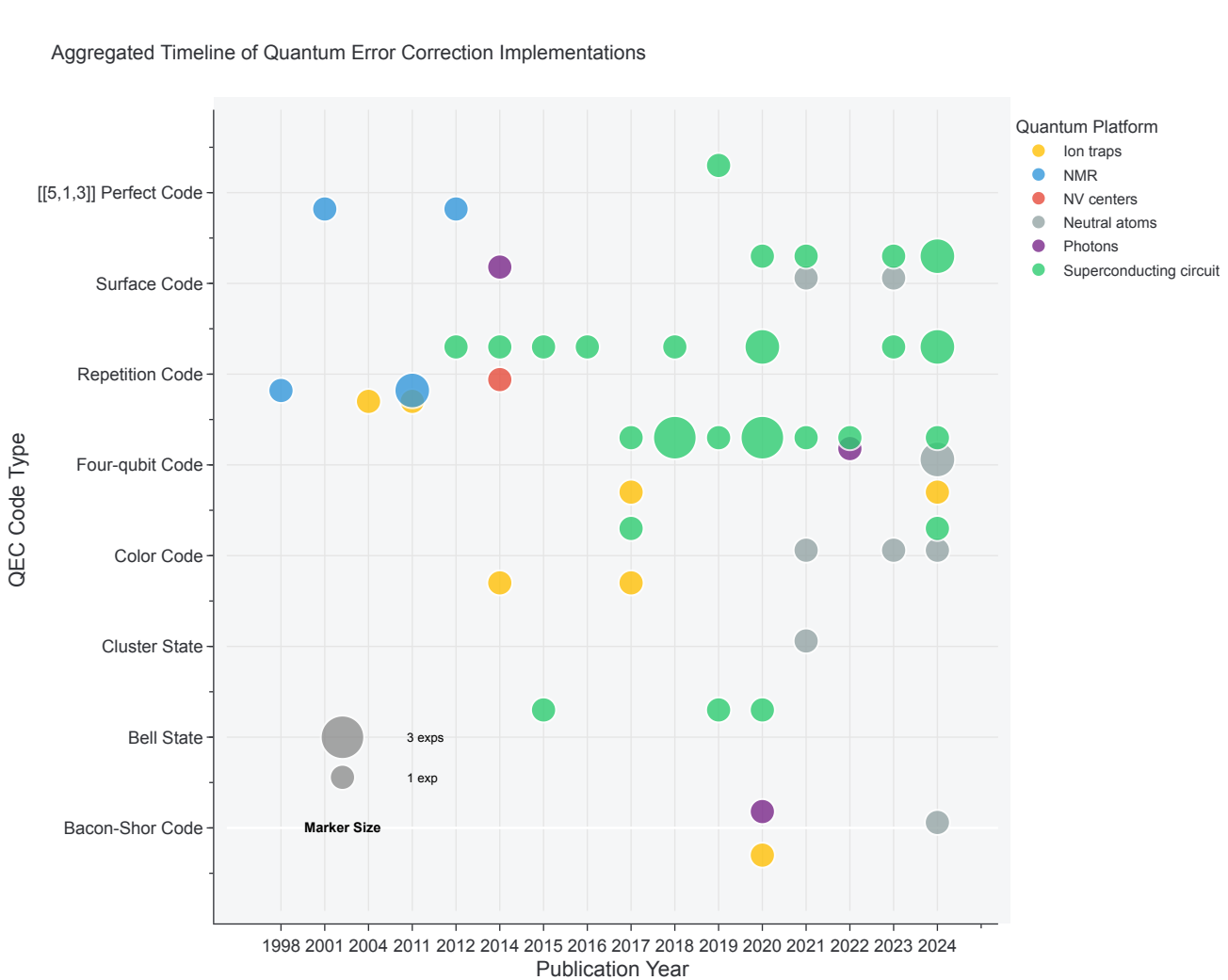


**Figure 8: Timeline of QEC Implementations.** Each point represents a reported experimental implementation of a specific QEC code type (y-axis) on a particular quantum platform (color/shape) in a given publication year (x-axis).

`scipy.stats.linregress` function from the SciPy library [179]. This function calculates the best-fit line parameters (slope  $m$  and intercept  $c$ ) and also returns the Pearson correlation coefficient, denoted as  $r$ .

The goodness of fit for this linear regression in log-space is quantified by the coefficient of determination,  $R^2$ , which is simply the square of the Pearson correlation coefficient ( $R^2 = r^2$ ). The  $R^2$  value represents the proportion of the variance in the dependent variable ( $\log_{10}(\text{metric})$ ) that is predictable from the independent variable (year). An  $R^2$  value ranges from 0 to 1, where 1 indicates that the linear model perfectly explains the variance in the transformed data (corresponding to a perfect exponential fit for the original data), and 0 indicates no linear correlation. Values close to 1 suggest that the exponential model provides a good description of the observed historical trend.

### 7.3.2 Results

The calculated  $R^2$  values obtained from the linear regression fits performed for Figure 1, Figure 2, Figure 3, are summarized in Table 3 below. Fits were only calculated where sufficient data points (at least three) were available for a given platform and metric.

Distribution of QEC Implementations Across Platforms



Figure 9: **Distribution of QEC Implementations Across Platforms.** Sunburst chart showing the breakdown of reported QEC code implementations (inner ring) by the physical platform used (outer ring). Numbers indicate the count of publications in the [qec\\_exp](#) database.

Table 3: **Goodness of Fit ( $R^2$ ) for Exponential Trends.** Note the lower fit quality for neutral atoms  $T_1$  corresponding to the different atomic species (Rubidium, Cesium, and Strontium) and superconducting circuits  $T_2$  due to the different implementations (transmons vs cavities).

Metric	Platform	$R^2$	Time Scale	Std Error
Coherence Time ( $T_1$ )	Semiconductor	0.954	$\times 2$ every 0.86y	0.077
	Superconducting circuit	0.809	$\times 2$ every 0.99y	0.032
	Neutral atoms	0.122	$\times 2$ every 5.89y	0.079
Coherence Time ( $T_2$ )	Neutral atoms	0.880	$\times 2$ every 2.38y	0.033
	Ion traps	0.860	$\times 2$ every 1.92y	0.045
	Superconducting circuit	0.418	$\times 2$ every 1.94y	0.045
Entanglement Error	Semiconductor spins	0.981	$\div 2$ every 1.16y	0.036
	Ion traps	0.952	$\div 2$ every 2.40y	0.011
	Superconducting circuits	0.933	$\div 2$ every 2.56y	0.016
Physical Qubit Count	Neutral atoms	0.889	$\div 2$ every 2.30y	0.015
	Semiconductor spins	0.983	$\times 2$ every 2.62y	0.015
	Ion traps	0.955	$\times 2$ every 5.03y	0.007

Metric	Platform	R <sup>2</sup>	Time Scale	Std Error
	Neutral atoms	0.948	$\times 2$ every 1.37y	0.019
	Superconducting circuit	0.877	$\times 2$ every 2.58y	0.025

### 7.3.3 Discussion

The  $R^2$  values presented in Table 3 are generally high (many above 0.85), suggesting that the exponential model captures a significant portion of the variance in the historical trends for most platforms and metrics analyzed. This supports the visual impression from Figure 1, Figure 2, Figure 3 and provides quantitative justification for using exponential fits to characterize the rates of progress (doubling/halving times).

However, certain caveats should be noted:

- The  $R^2$  value for Superconducting Circuit  $T_2$  time (0.418) is notably lower than others, reflecting that we included different families of implementations within the “superconducting qubits” category (transmons vs cavities), and an outlier with particularly small  $T_2$  breaks the exponential fit for this platform.
- Similarly, the lower  $R^2$  value for Neutral atoms  $T_1$  (0.122) reflects the inclusion of different atomic species (Rubidium, Cesium, and Strontium) with inherently different characteristics.
- A high  $R^2$  value confirms that the exponential model fits the historical data well but does not guarantee that the trend will continue into the future, as discussed in Section 7.1 regarding the limitations of extrapolation.

Overall, the analysis of  $R^2$  values reinforces the observation of strong historical exponential trends in key physical qubit metrics across major platforms, while also highlighting specific cases where the model fit is weaker or based on limited data.